Supporting Information

C-H Bond Activation via Concerted Metalation-Deprotonation at a Palladium(III) Center

Bailey Bouley,[1] Fengzhi Tang,[2] Dae Young Bae,[1] and Liviu M. Mirica[1,*]

[1] Department of Chemistry, University of Illinois at Urbana-Champaign, 505 S Mathews Ave, Urbana, IL 61801-3617,
[2] Department of Chemistry, Washington University, One Brookings Drive, St. Louis, MO 63130-4899.

Table of Contents

I. General Specifications

All operations were performed under a nitrogen atmosphere using standard Schlenk and glove box techniques if not indicated otherwise. All reagents for which the syntheses are not given were purchased from Sigma-Aldrich, Acros, STREM, or Pressure Chemical and were used as received without further purification. Solvents were purified prior to use by passing through a column of activated alumina using an MBRAUN SPS. N,N'-methyl-2,11-diaza[3,3](2,6)pyridinophane (^{Me}N4),[1] neophyl-Cl-d_5,[2] (COD)Pd(neophyl)Cl, (COD)Pd(neophyl-d_5)Cl,[3] (COD)Pd(cycloneophyl)[4], and AgOPiv[5] were prepared according to literature procedures. ^{1}H NMR spectra were obtained on a Varian Mercury-300 spectrometer (300.121 MHz) or a Bruker Ascend-600 spectrometer (600.13 MHz). ^{13}C NMR spectra were obtained on a Bruker Ascend-600 spectrometer (150.92 MHz). Cyclic voltammetry (CV) studies were performed with a BASi EC Epsilon electrochemical workstation. The reference electrodes were calibrated against ferrocene at the end of each CV measurement. Chemical shifts are reported in parts per million (ppm) with residual solvent resonance peaks as internal references.[6] Abbreviations for the multiplicity of NMR signals are singlet (s), doublet (d), triplet (t), quartet (q), septet (sep), multiplet (m), broad resonance (br). UV-visible spectra were recorded on a Varian Cary 50 Bio spectrophotometer and are reported as λ_{max}, nm (λ, $M^{-1}cm^{-1}$). EPR spectra were recorded on a JEOL JES-FA X-band (9.2 GHz) EPR spectrometer in PrCN-MeCN (3:1) at 77 K. ESI-MS experiments were performed using a linear quadrupole ion trap Fourier transform ion cyclotron resonance mass spectrometer (LTQ-FTMS, Thermo, San Jose, CA) or a Bruker Maxis Q-TOF mass spectrometer with an electrospray ionization source. ESI mass-spectrometry was provided by the Washington University Mass Spectrometry Resource. Elemental analyses were carried out by the Intertek Pharmaceutical Services.

II. Synthesis of Pd Complexes

(^{Me}N4)Pd^{II}(neophyl)Cl (1)

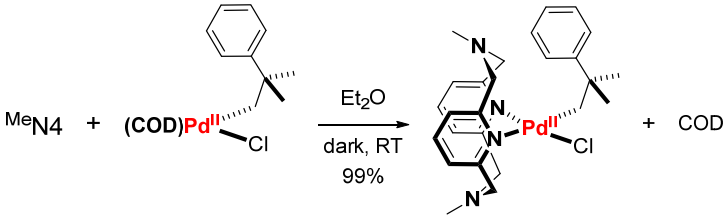

1

Under nitrogen, ^{Me}N$_4$ (59.6 mg, 0.222 mmol) and (COD)Pd^{II}(neophyl)Cl (85.2 mg, 0.222 mmol) were loaded in a round bottom flask. Then, anhydrous diethyl ether (15 mL) was added to form a yellowish suspension. This suspension was allowed to stir for two days in the absence of light. The generated pale-yellow precipitate was filtered off, washed with ether and pentane, and dried *in vacuo*. The product (^{Me}N4)Pd^{II}(neophyl)Cl was isolated as a pale yellow solid. Yield: 120 mg, 99 % yield.

Anal. Found: C, 57.22; H, 5.80; N, 10.84; Calcd for (^{Me}N4)Pd^{II}(neophyl)Cl (C26H33ClN4Pd) : C, 57.46; H, 6.12; N, 10.31.

^{1}H NMR (600 MHz, CD_3CN) δ 7.47 (br, 1H, py-H), 7.41 (br, 1H, py-H), 7.10 (d, J = 7.7 Hz, 2H, ph-H), 6.99 (br, 2H, py-H), 6.95 – 6.85 (m, 5H, py-H and ph-H), 6.02 (d, J = 12.2 Hz, 2H, -CH_2-), 5.49 (d, J = 13.0 Hz, 2H, -CH_2-), 4.06 (d, J = 13.4 Hz, 2H, -CH_2-), 3.78 (d, J = 13.8 Hz, 2H, -CH_2-), 2.45 (s, 2H, Pd-CH_2), 2.16 (s, 6H, N-CH_3), 1.32 (s, 6H, C(CH_3)$_2$).

^{1}H NMR (600 MHz, CD_2Cl_2) δ 7.38 (br, 1H, py-H), 7.34 (br, 1H, py-H), 7.07 (d, J = 6.1 Hz, 2H), 6.95 – 6.83 (m, 5H, py-H and ph-H), 6.78 (br, 2H), 6.11 (br, 2H, -CH_2-), 5.57 (br, 2H, -CH_2-), 4.03 (br, 2H, -CH_2-), 3.74 (br, 2H, -CH_2-), 2.50 (s, 2H, Pd-CH_2), 2.19 (s, 6H, N-CH_3), 1.37 (s, 6H, C(CH_3)$_2$).

^{13}C NMR (151 MHz, CD_2Cl_2) δ 159.10, 157.35, 151.44, 136.77, 136.35, 127.79, 126.04, 124.90, 124.73, 66.32, 63.69, 41.46, 39.65, 32.66, 26.98.

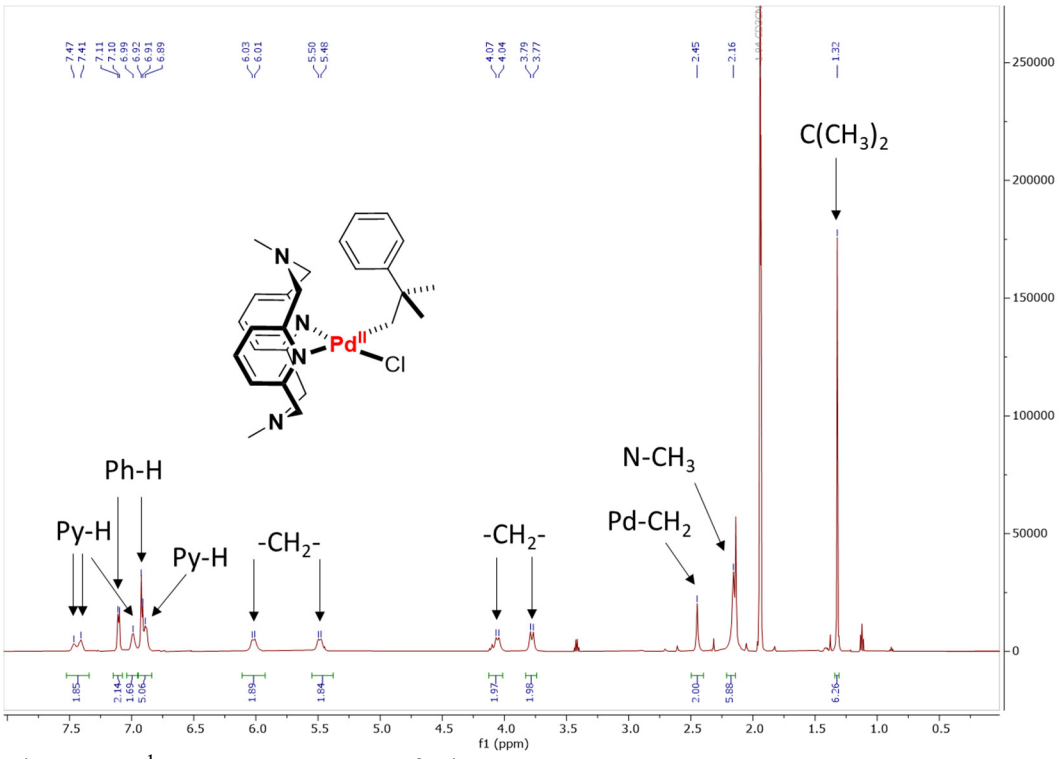

Figure S1. ^{1}H NMR spectrum of **1** in CD_3CN.

(^{Me}N4)Pd^{II}(neophyl-d_5)Cl (**1**-d_5) was synthesized by reacting ^{Me}N4 (39.6 mg, 0.15 mmol) with 1 equiv. of (COD)Pd^{II}(neophyl-d_5) (57.3 mg, 0.15 mmol) by a similar procedure. Yield: 72.8 mg, 90%.

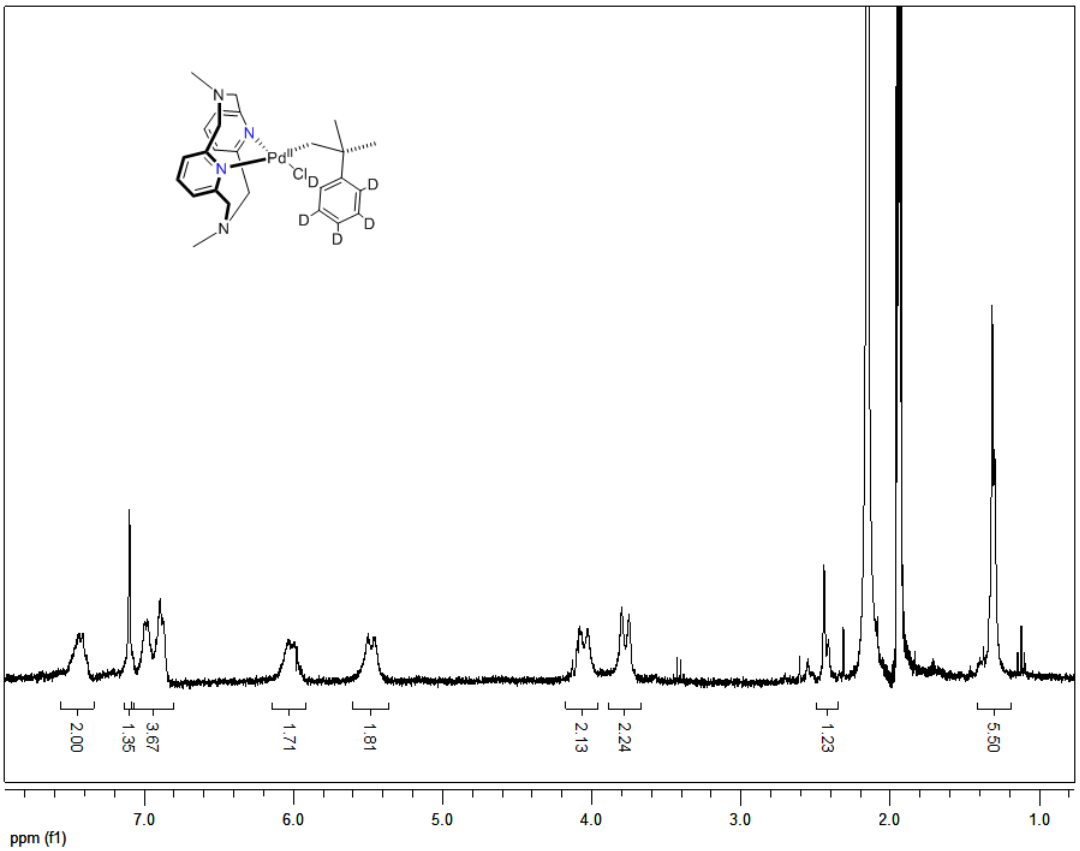

Figure S2. ^{1}H NMR spectrum of **1**-d_5 in CD_3CN. Note: the slightly lower integration for the methylene peak (2.45 ppm) and methyl peak (1.32 ppm) of the neophyl ligand is due to the integration of deuterium during the synthesis of (COD)Pd(neophyl-d_5)Cl.

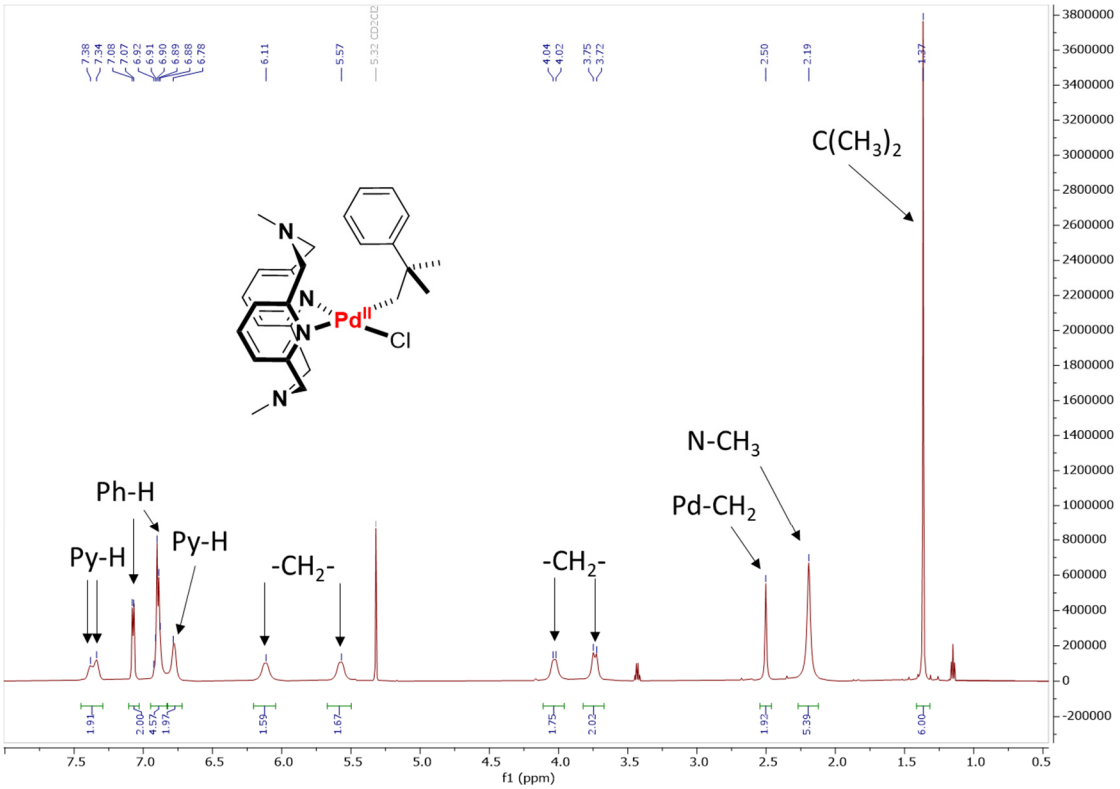

Figure S3. ^{1}H NMR of **1** in CD_2Cl_2.

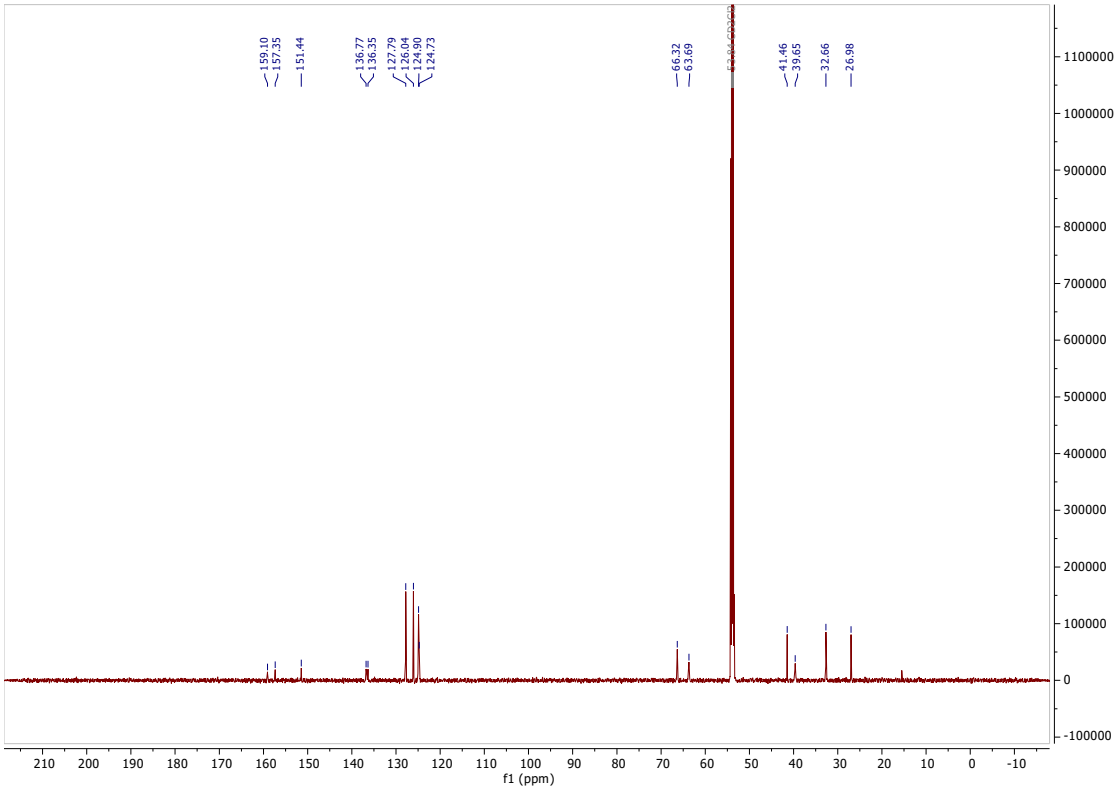

Figure S4. ^{13}C NMR of **1** in CD_2Cl_2.

(^{Me}N4)Pd^{II}(cycloneophyl) (2)

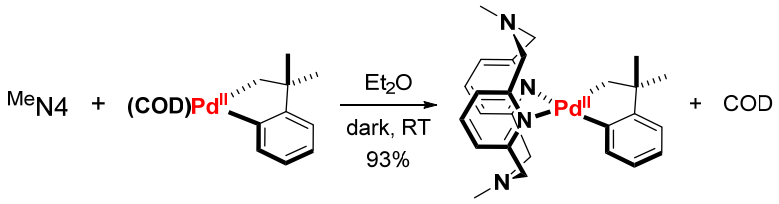

2

Under nitrogen, $^{Me}N_4$ (62.7 mg, 0.234 mmol) and (COD)Pd^{II}(cycloneophyl) (81.0 mg, 0.234 mmol) were loaded in a round bottom flask. Then anhydrous diethyl ether (15 mL) was added to form a white suspension. This suspension was allowed to stir for two days in the absence of light. Then, the generated white precipitate was filtered off, washed with ether and pentane, and dried *in vacuo*. The product (^{Me}N4)Pd^{II}(cycloneophyl) was isolated as a white solid. Yield: 110 mg, 93 % yield.

Anal. Found: C, 61.22; H, 5.80; N, 10.84; Calcd for (^{Me}N4)Pd^{II}(cycloneophyl) (C26H32N4Pd) : C, 61.60; H, 6.36; N, 11.05. Note: This compound is very unstable, undergoes thermal decomposition at room temperature.

^{1}H NMR (300MHz, CD_3CN), δ: 7.55 (m, 2H, py-H), 7.10 (m, 4H, py-H), 6.74 (m, 2H, Ph-H), 6.52 (m, 2H, Ph-H), 5.98 (d, 4H, J = 12.9 Hz, -CH_2-), 4.11(d, 4H, J = 13.5 Hz, -CH_2-), 2.32 (s, 6H, N-CH_3), 2.05 (s, 2H, Pd-CH_2), 1.38 (s, 6H, CH_3).

^{13}C NMR (151 MHz, CD_3CN) δ 168.68, 160.61, 158.59, 158.29, 137.02, 135.95, 125.52, 125.36, 124.35, 123.21, 122.59, 64.39, 49.03, 40.24, 39.25, 34.11.

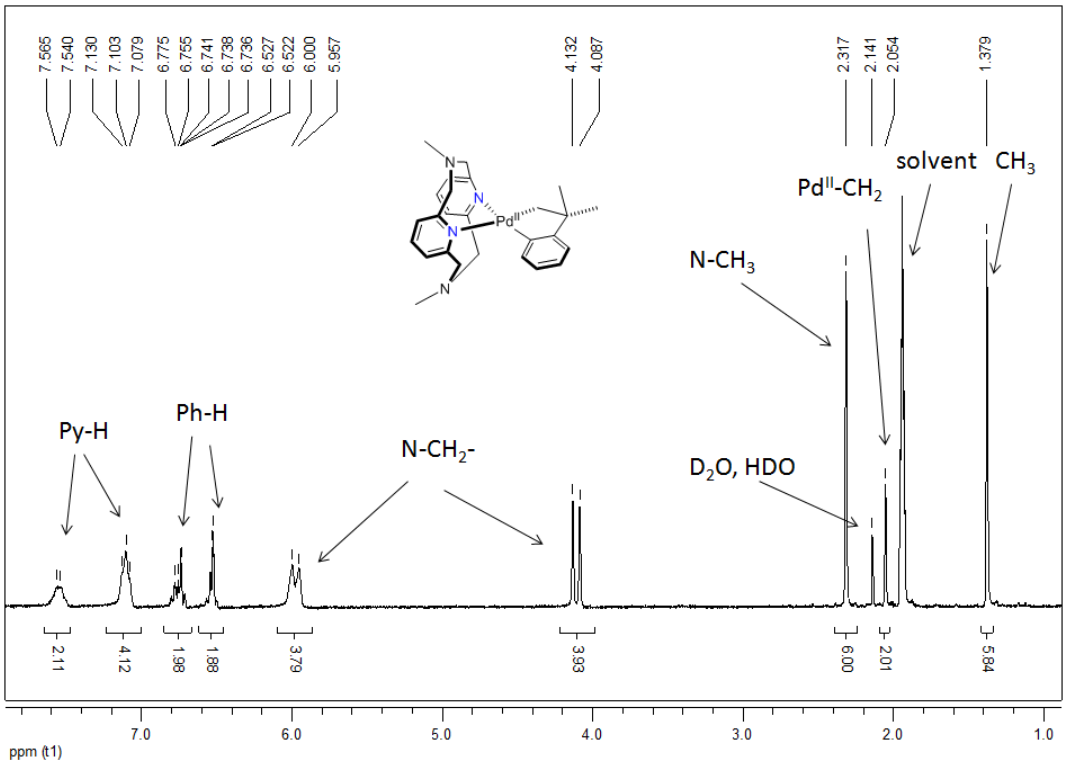

Figure S5. ^{1}H NMR spectrum of **2** in CD_3CN.

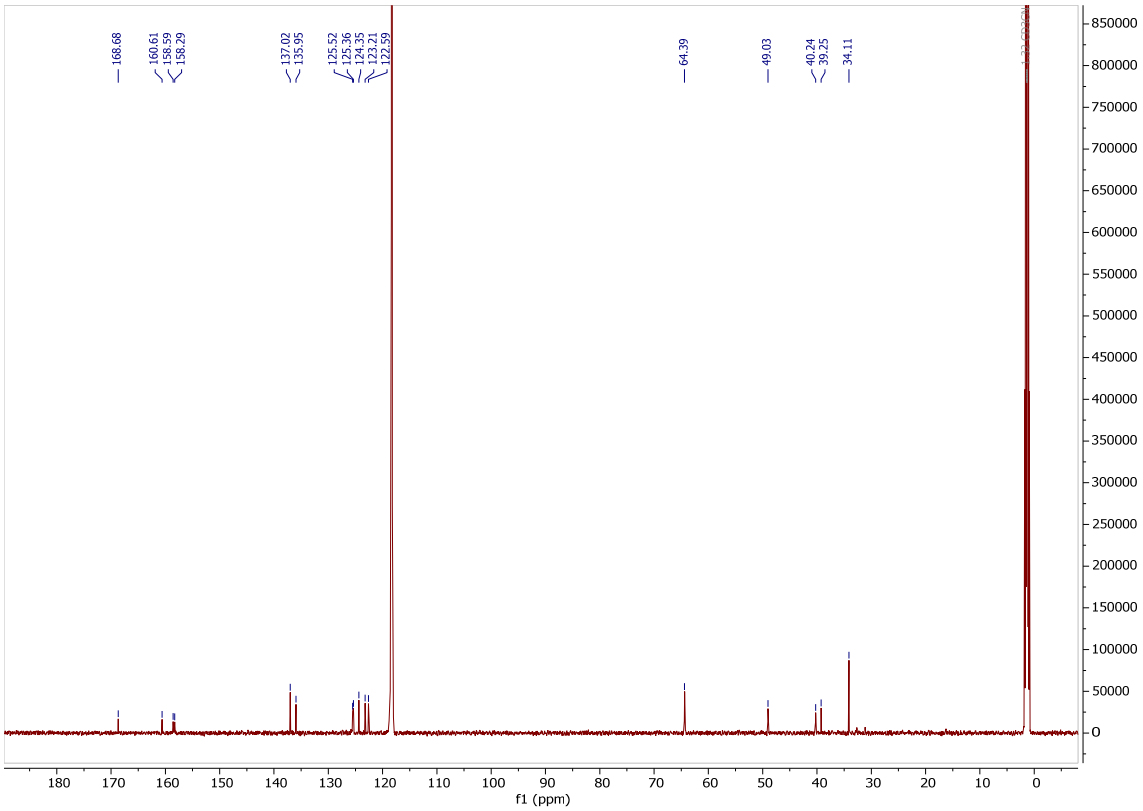

Figure S6. ^{13}C NMR of **2** in CD_3CN.

[(^{Me}N4)Pd^{III}(neophyl)Cl] ([1^{+}])

In a N_2 filled glove box, complex **1** (27.2 mg, 0.05 mmol) and 1 equiv. of $FcPF_6$ (16.6 mg, 0.05 mmol) were mixed in MeCN (5 mL) for 30 min. Then the dark purple solution was concentrated to about 2 mL, washed with pentane (3 x 4 mL), and dried completely under vacuum. Yield: 32 mg, 99 %. For crystallization, the dark purplish residue was re-dissolved in THF (2 mL), and to this solution, 4 equiv. of $LiClO_4$ (21.2 mg, 0.2 mmol) was added, and the mixture was filtered. Diffusion of diethyl ether at -35 ºC yielded dark purple crystals after a couple of days. Those crystals were isolated, washed with ether and pentane, and dried under high vacuum. Yield: 15.2 mg, 47 %.

EA analysis. Anal. Found: C, 40.21; H, 4.57; N, 6.46; Calcd for [(^{Me}N$_4$)Pd^{III}(neophyl)Cl]ClO_4•$LiClO_4$•2H_2O: ($C_{26}H_{37}N_4Cl_3O_{10}LiPd$): C, 39.76; H, 4.75; N, 7.13.

UV-Vis: 625 nm (540 $M^{-1}cm^{-1}$), 494 nm (440 $M^{-1}cm^{-1}$), 324 nm (4750 $M^{-1}cm^{-1}$).

ESI-MS of solution of [(^{Me}N4)Pd^{III}(neophyl)Cl]$^{+}$ in MeCN, m/z 542.1421; calculated for $[C_{18}H_{24}N_6PdO_4]^{+}$ 542.1429.

[(^{Me}N4)Pd^{III}(cycloneophyl)]ClO$_4$ ([2$^+$]ClO$_4$)

In a N_2 filled glove box, complex **2** (10.0 mg, 0.02 mmol) and 1 equiv. of $FcPF_6$ (6.5 mg, 0.02 mmol) were mixed in MeCN (3 mL) for 30 min. Then the dark green solution was concentrated to about 1 mL and washed with pentane (3 x 3 mL). For crystallization, 4 equiv. of $LiClO_4$ (8.5 mg, 0.02 mmol) was added and the mixture was filtered. Diffusion with diethyl ether at -35 ºC yielded dark green crystals after a couple of days. Those crystals were isolated, washed with ether and pentane, and dried under high vacuum. Yield: 4.2 mg, 35 %.

EA analysis. Anal. Found: C, 51.78; H, 5.66; N, 8.99; Calcd for [(^{Me}N$_4$)Pd^{III}(cycloneophyl)]ClO$_4$: ($C_{26}H_{32}N_4ClO_4Pd$): C, 51.49; H, 5.32; N, 9.24.

UV-Vis: 675 nm (425 $M^{-1}cm^{-1}$), 500 nm (shoulder, 520 $M^{-1}cm^{-1}$), 335 nm (2800 $M^{-1}cm^{-1}$).

ESI-MS of solution of [(^{Me}N4)Pd^{III}(cycloneophyl)]$^+$ in MeCN, m/z 506.1641; calculated for $[C_{18}H_{24}N_6PdO_4]^+$ 506.1642.

[(^{Me}N4)Pd^{IV}(cycloneophyl)](ClO$_4$)$_2$ ([2^{2+}](ClO$_4$)$_2$)

In a N_2 filled glove box, complex **2** (15.0 mg, 0.03 mmol) and 2 equiv. of $FcPF_6$ (19.6 mg, 0.06 mmol) were mixed in MeCN (3 mL) for 30 min. The resulting orange solution was concentrated to about 1 mL and washed with pentane (3 x 3 mL). For crystallization, 4 equiv. of $LiClO_4$ (12.8 mg, 0.12 mmol) was added, and the mixture was filtered. Diffusion of diethyl ether at -35 ºC yielded orange crystals after a couple of days. Those crystals were isolated, washed with ether and pentane, and dried under high vacuum. Yield: 14.5 mg, 68 %.

EA analysis. Anal. Found: C, 44.12; H, 4.87; N, 7.45; Calcd for [(^{Me}N$_4$)Pd^{IV}(cycloneophyl)](ClO$_4$)$_2$: ($C_{26}H_{32}N_4O_8Cl_2Pd$): C, 44.24; H, 4.57; N, 7.94.

ESI-MS of solution of [(^{Me}N4)Pd^{IV}(cycloneophyl)]$^{2+}$ in MeCN, m/z 253.0835; calculated for $[C_{18}H_{24}N_6PdO_4]^+$ 253.0837.

^{1}H NMR (300MHz, CD_3CN), δ: 7.99 (t, 1H, *J* = 7.8 Hz, py-H), 7.93 (t, 1H, *J* = 7.8 Hz, py-H), 7.49 (d, 2H, *J* = 7.8 Hz, py-H), 7.40 (d, 2H, *J* = 7.8 Hz, py-H), 7.28 (m, 2H, Ph-H), 7.02 (d, 2H, *J* = 3.0 Hz Ph-H), 5.28 (d, 2H, *J* = 16.2 Hz, -CH_2-), 5.02 (d, 2H, *J* = 16.2 Hz, -CH_2-), 4.57 (d, 2H, *J* = 16.2 Hz, -CH_2-), 4.50 (d, 2H, *J* = 16.2 Hz, -CH_2-), 4.31 (s, 2H, Pd-CH_2), 2.86 (s, 6H, N-CH_3), 1.63 (s, 6H, CH_3).

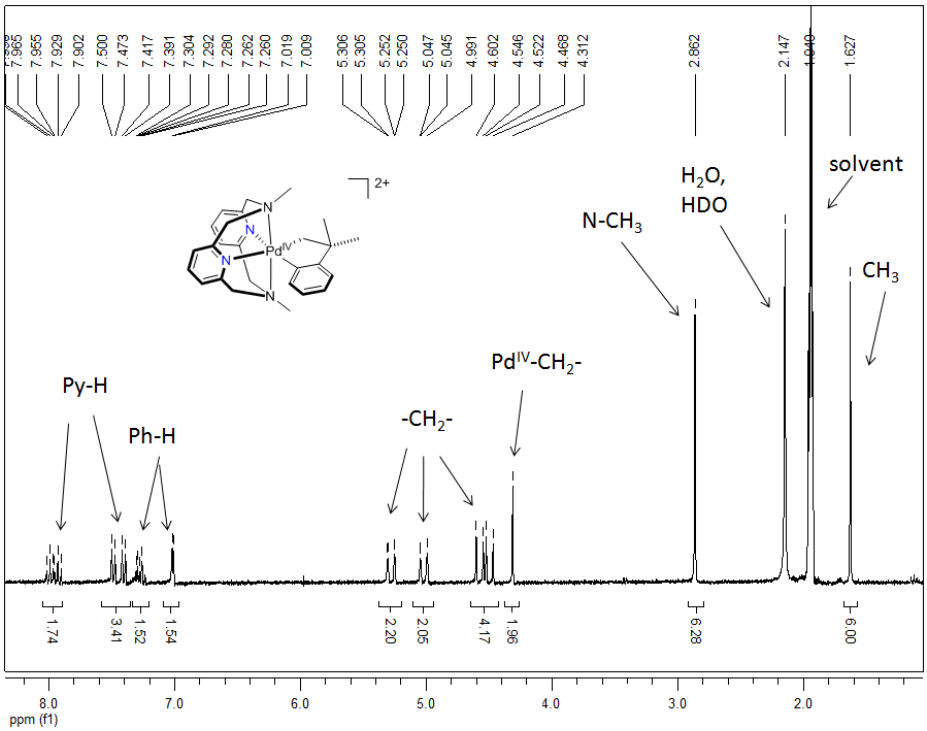

Figure S7. ^{1}H NMR spectrum of [$\mathbf{2}^{2+}$]$(ClO_4)_2$ in CD_3CN.

Attempts of preparing [(^{Me}N4)Pd^{IV}(neophyl)Cl](ClO$_4$)$_2$

In a N_2 filled glove box, complex **1** (22.8 mg, 0.04 mmol) and 2 equiv. of $NOBF_4$ (9.8 mg, 0.08 mmol) were mixed in CD_3CN (1 mL). While an NMR spectrum of the resulting Pd^{IV} species could be obtained, the complex was not stable for long periods of time and could not be isolated. Alternatively, the isolated complex [($^{Me}N_4$)Pd^{III}(neophyl)Cl]ClO_4 could be used and addition of 1 equiv. of $NOBF_4$ in CD_3CN (1 mL) generated an identical NMR spectrum.

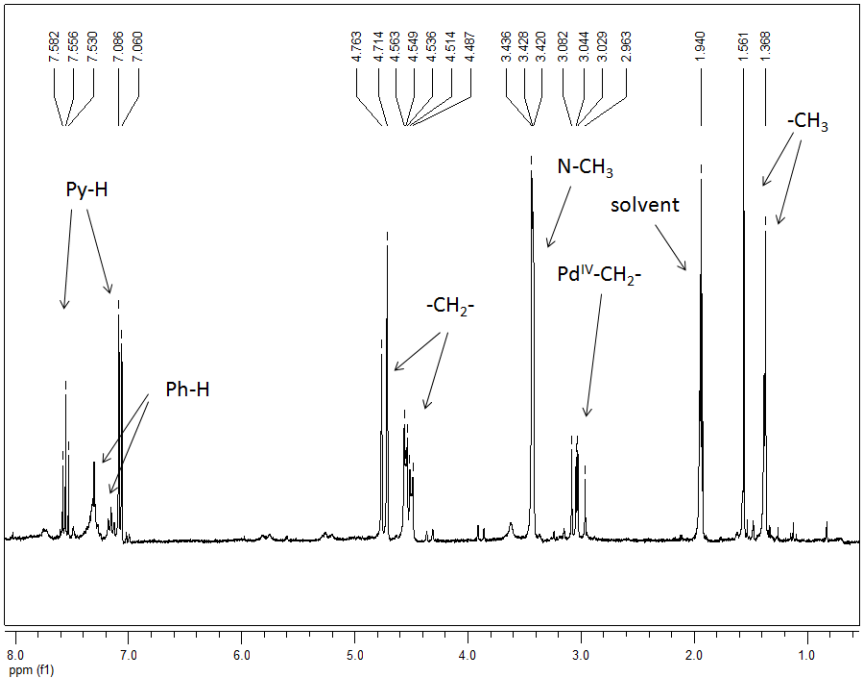

Figure S8. ^{1}H NMR spectrum of mixture of complex **1** and 2 equiv. of $NOBF_4$ in CD_3CN after 30 min.

III. C-H activation studies at Pd^{III} species

UV-Vis studies

In a 20 mL vial, $\mathbf{1}^+$ (5.4 mg, .008 mmol) was dissolved in 6 mL MeCN to which 1 equiv. of AgOAc (1.3 mg, 0.008 mmol) was added while stirring. At each time point, 500 µL of the solution was removed and filtered through a syringe filter to remove precipitated silver chloride into a 1 mL, 1 cm path length cuvette for UV-Vis analysis. The transformation of $\mathbf{1}^+$ to $\mathbf{2}^+$ was monitored by the disappearance of the band at 625 nm and the appearance of the band at 675 nm corresponding to the formation of $\mathbf{2}^+$. The reaction was complete after 3 hours with no more change in the intensity of the 675 nm band. Yield: 44%.

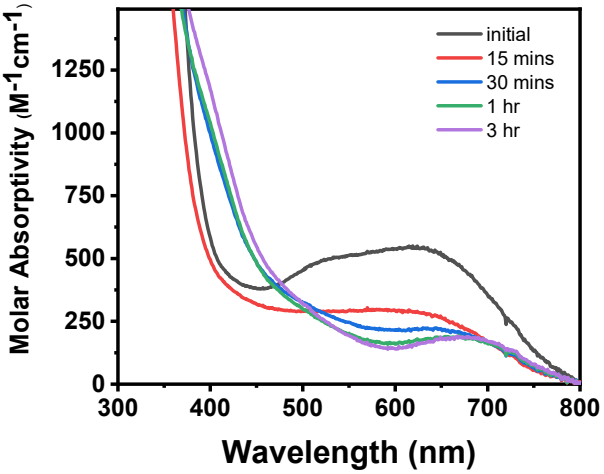

Figure S9. UV-Vis spectra showing the transition of $\mathbf{1}^+$ to $\mathbf{2}^+$ in the presence of 1 equiv. of AgOAc.

EPR studies

In a 7.0 mL vial equipped with a magnetic stir bar and a Teflon-lined cap, complex **1** (5.4 mg, 0.01 mmol) and 1 equiv. of $FcPF_6$ (3.3 mg, 0.01 mmol) were mixed in MeCN (2.5 mL) and stirred for 15 min to make a 4.0 mM $[\mathbf{1}^+]PF_6$ solution in situ. Then, a 100 µL aliquot of the reaction mixture was taken by pipette and diluted 4 times with PrCN (300 µL). This mixture was transferred to an EPR tube and frozen with liquid nitrogen immediately for EPR measurement. To the remaining reaction mixture, 1 equiv. of AgOAc (1.7 mg, 0.01 mmol) was added and reaction was stirred rapidly. At time points 1 min, 5 min, 10 min, 15 min, 20 min, 30 min, 50 min, 110 min, 280 min, and 460 min, a 100 µL aliquot of the reaction mixture was taken by pipette, diluted 4 times with PrCN (300 µL), frozen by liquid nitrogen, and tracked by EPR spectroscopy.

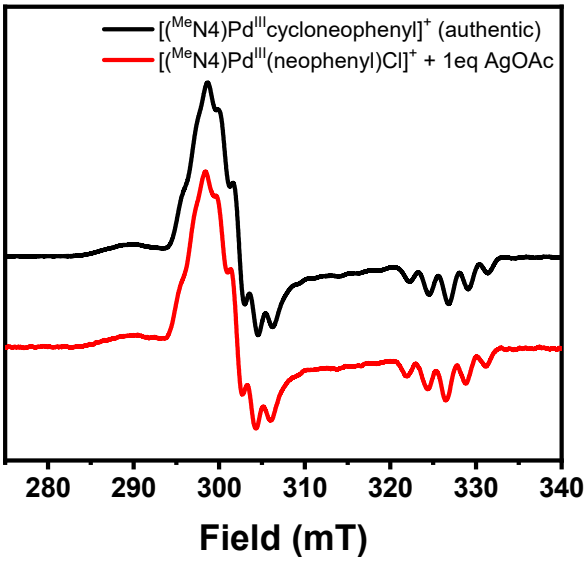

Figure S10. EPR spectra of the independently synthesized $\mathbf{2}^{+}$ and C-H activation product at Pd^{III} center of $\mathbf{1}^{+}$ promoted by AgOAc.

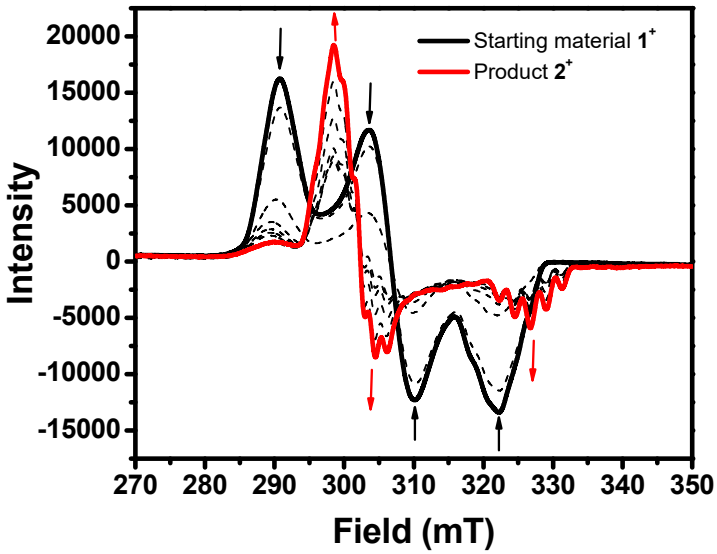

Figure S11. EPR spectra of the reaction mixture of $\mathbf{1}^{+}$ and 1 equiv. of AgOAc in MeCN at room temperature.

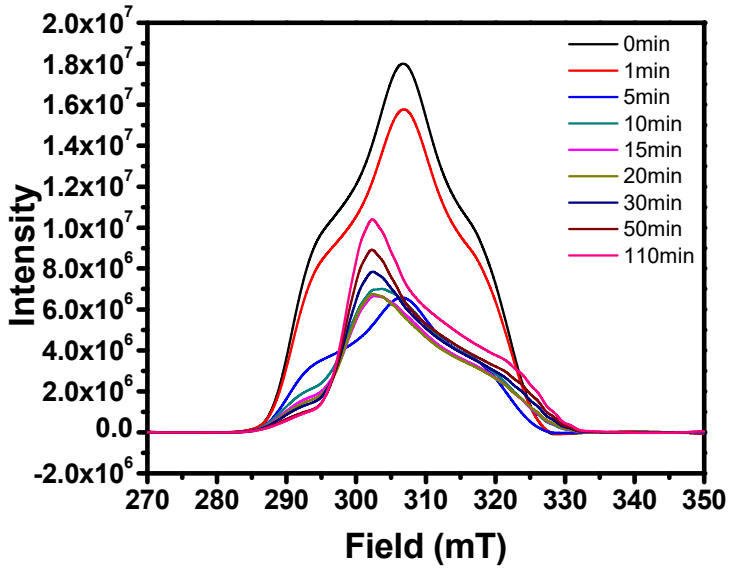

Figure S12. The integration of the EPR spectra of reaction mixture of $\mathbf{1}^+$ and 1 equiv. of AgOAc in MeCN at room temperature.

Table S1. Spin area based on the double integration of EPR spectra of various time points. The spin area percentages are relative to the 0 min time point.

Time (min)	0	1	5	10	15	20	30	50	110	280
Relative spin area (%)	100	87.6	36.9	38.4	35.4	34.9	38.7	41.2	47.4	44.56

Control experiments with separate Ag^+ or OAc^- sources

Control experiment $\mathbf{1}^+$ + $AgBF_4$: In a 20 mL vial, $\mathbf{1}^+$ (5.4 mg, 0.008 mmol) was dissolved in MeCN (6 mL) to which 1 equiv. of $AgBF_4$ (1.3 mg, 0.008 mmol) was added while stirring. At each time point, 500 µL of the solution was removed and filtered through a syringe filter to remove precipitated silver chloride into a 1 mL, 1 cm path length cuvette for UV-Vis analysis. The generation of a new band in the UV-Vis spectrum at 560nm is assigned to the acetonitrile adduct: $^{Me}N4Pd^{III}$(neophyl)(MeCN).

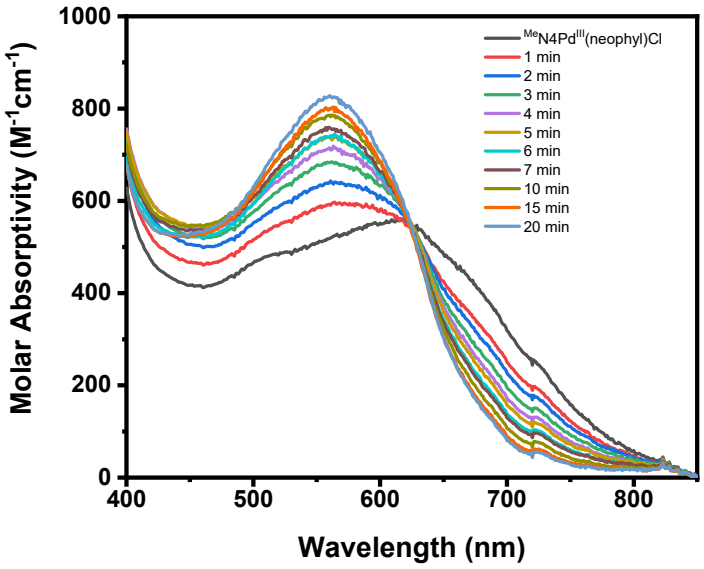

Figure S13. UV-Vis spectra of reaction mixture of $\mathbf{1}^+$ and 1 equiv. of $AgBF_4$ in MeCN at room temperature at various time points. Note: the AgCl precipitate was filtered away prior to measurement.

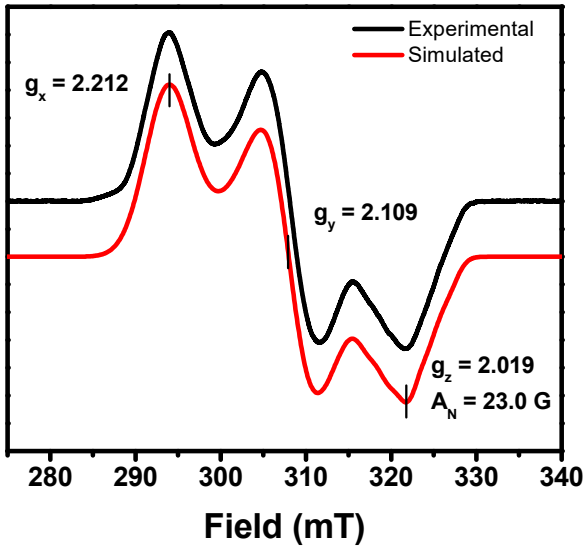

Figure S14. EPR spectrum of complex $[\mathbf{1}^+]ClO_4$ with 1 equiv. $AgBF_4$ in 3:1 PrCN/MeCN. $g_x = 2.212$, $g_y = 2.109$, $g_z = 2.019$ ($A_N = 23.0$ G).

Control experiment 1^+ + OAc^-: In a 7.0 mL via equipped with a magnetic stir bar and a Teflon-lined cap, complex **1** (5.4 mg, 0.01 mmol) and 1 equiv. of $FcPF_6$ (3.3 mg, 0.01 mmol) were mixed in MeCN (2 mL) and stirred for 15 min. Then, 4 equiv. of $Et_4NOAc•4H_2O$ (10.5 mg, 0.04 mmol) was added to the reaction mixture. Then the solution was diluted 10 times and the reaction was followed by UV-Vis. Based on the absorbance of peak at 675 nm, cyclometalated product $\mathbf{2}^+$ was generated slowly and reached the maximum yield of 33% in 3h. Analogues reactions with up to 10 equiv. of $Et_4NOH•4H_2O$ were also performed, but less product $\mathbf{2}^+$ was observed as the starting material $\mathbf{1}^+$ slowly decayed. Similar reactions were performed with Bu_4NOAc as acetate source.

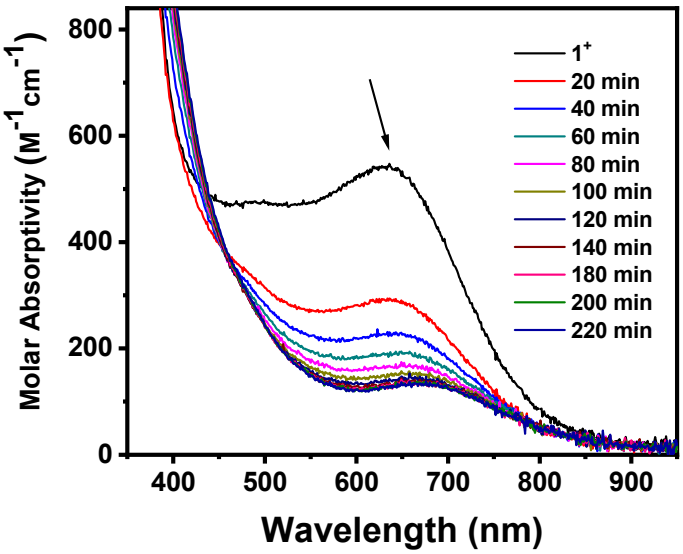

Figure S15. Formation of cyclometalated product $\mathbf{2}^+$ during C-H activation process of 0.5 mM $\mathbf{1}^+$ with 4 equiv. of Et_4NOAc in MeCN followed by UV-vis spectroscopy (Δt = 20 min, t = 0-220 min).

Table S2. Yields and reaction time for the reaction between complex $\mathbf{1}^+$ and carboxylate sources under different conditions.

Acetate source	Amount of acetate	Maximum yield of $\mathbf{2}^+$	Reaction time at maximum yield of $\mathbf{2}^+$
$Et_4NOAc•4H_2O$	1 equiv.	36%	1200 min
$Et_4NOAc•4H_2O$	4 equiv.	33%	220 min
$Et_4NOAc•4H_2O$	10 equiv.	< 5%	decay of $\mathbf{1}^+$ in a few minutes
Bu_4NOAc	1 equiv.	41%	1600 min
Bu_4NOAc	2 equiv.	34%	1100 min
Bu_4NOAc	5 equiv.	< 5%	decay of $\mathbf{1}^+$ in a few minutes
AgOPiv	1 equiv.	37%	360 min

Control experiment of reactions with a non-nucleophilic base: In a 20 mL vial, $\mathbf{1}^+$ (5.5 mg, 0.008 mmol) was dissolved in MeCN (6 mL) to which either 1 equiv. or 4 equiv. of 2,6-lutidine (0.86 µL or 3.42 µL, 0.008 mmol or 0.031 mmol) was added while stirring, and the reaction was tracked by UV-Vis over 3 hours and up to 72 hours. In no case was formation of $\mathbf{2}^+$ observed. An additional control experiment was performed in which 4 equiv. of 2,6-lutidine (3.42 µL, 0.031 mmol) was added to a solution of in situ generated **Int-A** from $\mathbf{1}^+$. Coincidently, no formation of $\mathbf{2}^+$ was observed.

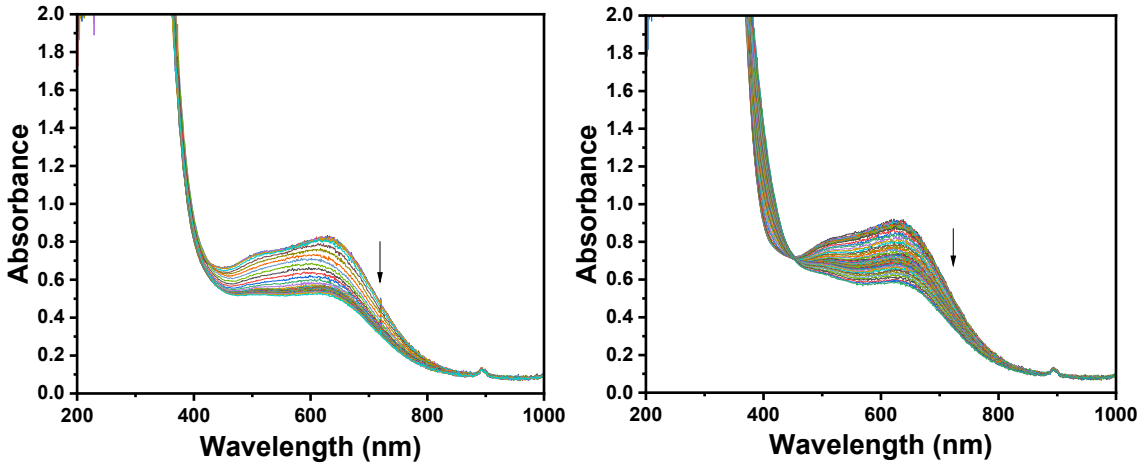

Figure S16. Addition of either 1 equiv. (left) or 4 equiv. (right) of 2,6-lutidine to $\mathbf{1}^+$ tracked by UV-Vis over 3 hours. No cyclometalated product was observed.

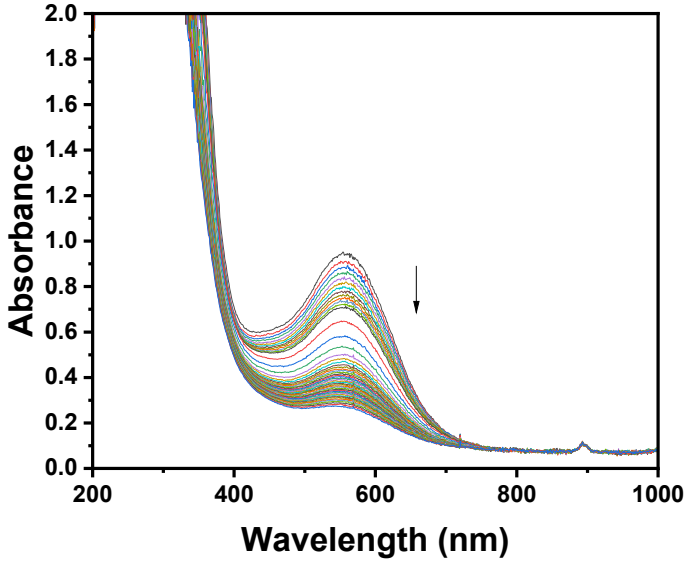

Figure S17. Addition of 4 equiv. of 2,6-lutidine to in-situ generated **Int-A** tracked by UV-Vis over 3 hours. No cyclometalated product was observed.

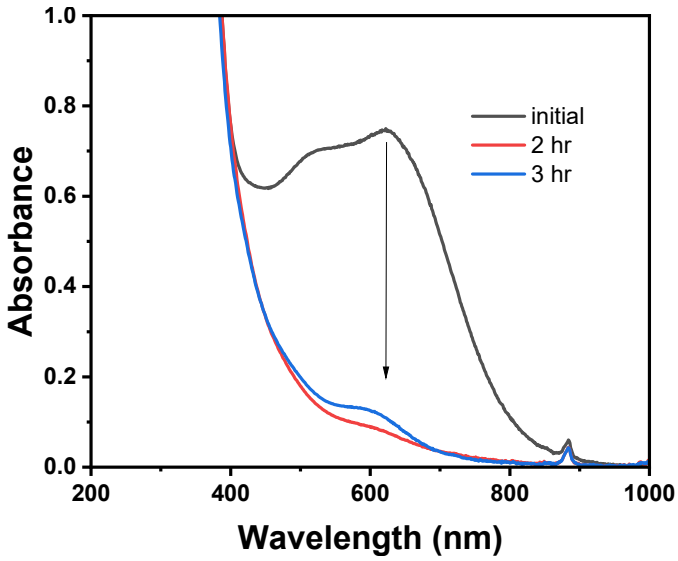

Figure S18. Reaction between $\mathbf{1}^{+}$ and 1 equiv. AgOAc in dichloromethane over 3 hours. No cyclometalated product was observed.

Control experiment at Pd^{II} oxidation state

In a 7.0 mL via equipped with a magnetic stir bar and a Teflon-lined cap, complex **1** (8.5 mg, 0.016 mmol) and 1 equiv. of AgOAc (2.61 mg, 0.016 mmol) were mixed in MeCN (3 mL). Aliquot samples were taken, filtered, and measured by UV-Vis at different time points. The same reaction was also performed in CD_3CN with trimethoxybenzene as an internal standard, and the reaction progress was followed by ^{1}H NMR.

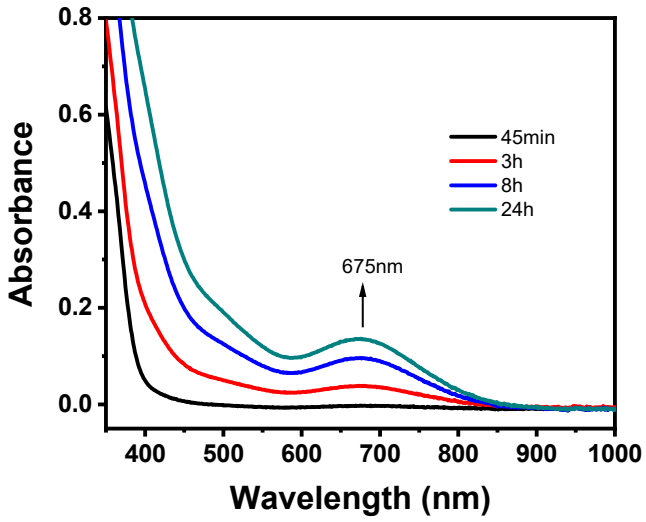

Figure S19. Formation of cyclometalated product $\mathbf{2}^{+}$ during the reaction of complex **1** with 1 equiv. of AgOAc in MeCN followed by UV-vis spectroscopy at different time points.

Table S3. Yields of the cyclometalated product **2** and $\mathbf{2}^+$ and starting material **1** left in the reaction of complex **1** with 1equiv. of AgOAc.

Time	**1**, %	**2**, %	$\mathbf{2}^+$, %
45 min	40	56	3
3 h	40	45	14
8 h	40	30	27
24 h	39	22	38

Control experiment: 1 + 2 eq $AgBF_4$

In a 7.0 mL via equipped with a magnetic stir bar and a Teflon-lined cap, complex **1** (5 mg, 0.01 mmol) and 1 equiv. of $AgBF_4$ (3.6 mg, 0.02 mmol) were mixed in CD_3CN (1 mL), and the starting material **1** decomposed quickly, and neither palladacycle **2** nor $\mathbf{2}^+$ (based on EPR) was formed.

Control experiment: 1 + 1 eq $Et_4OAc•4H_2O$

In a NMR tube, complex **1** (3.9 mg, 0.007 mmol) was mixed with 1 equiv. of $Et_4OAc•4H_2O$ (1.9 mg, 0.007 mmol) in CD_3CN (1 mL). The reaction mixture was followed by ^1H NMR periodically. Based on ^1H NMR, palladacycle **2** was yielded quantitatively

Control experiment: $[(^{Me}N4)Pd^{III}(neophyl)Cl]^+$ ($\mathbf{1}^+$) + 2eq AgOAc

In order to investigate the possible involvement of Pd^{IV} intermediate formation due to Ag^+ sources, in situ formed $\mathbf{1}^+$ was reacted with 2 equiv. of AgOAc. Complex **1** (2.3 mg, 0.004 mmol) was first reacted with 1 equiv. of $FcPF_6$ (1.4 mg, 0.004 mmol) in CD_3CN (1 mL) for 15 min to yield dark purplish Pd^{III} species $\mathbf{1}^+$. Then to this solution, 2 equiv. of AgOAc (1.4 mg, 0.008 mmol) was added, and the dark purplish solution first turn green (corresponding to $\mathbf{2}^+$) and then turned yellowish in about 30 min. Based on the chemical shift of the product, either $[^{Me}N4H]^+$ or the $[^{Me}N4Ag]^+$ species (based on both ^1H NMR and ESI-MS of the reaction mixture) and t-Butylbenzene were formed. No $\mathbf{2}^{2+}$ was observed.

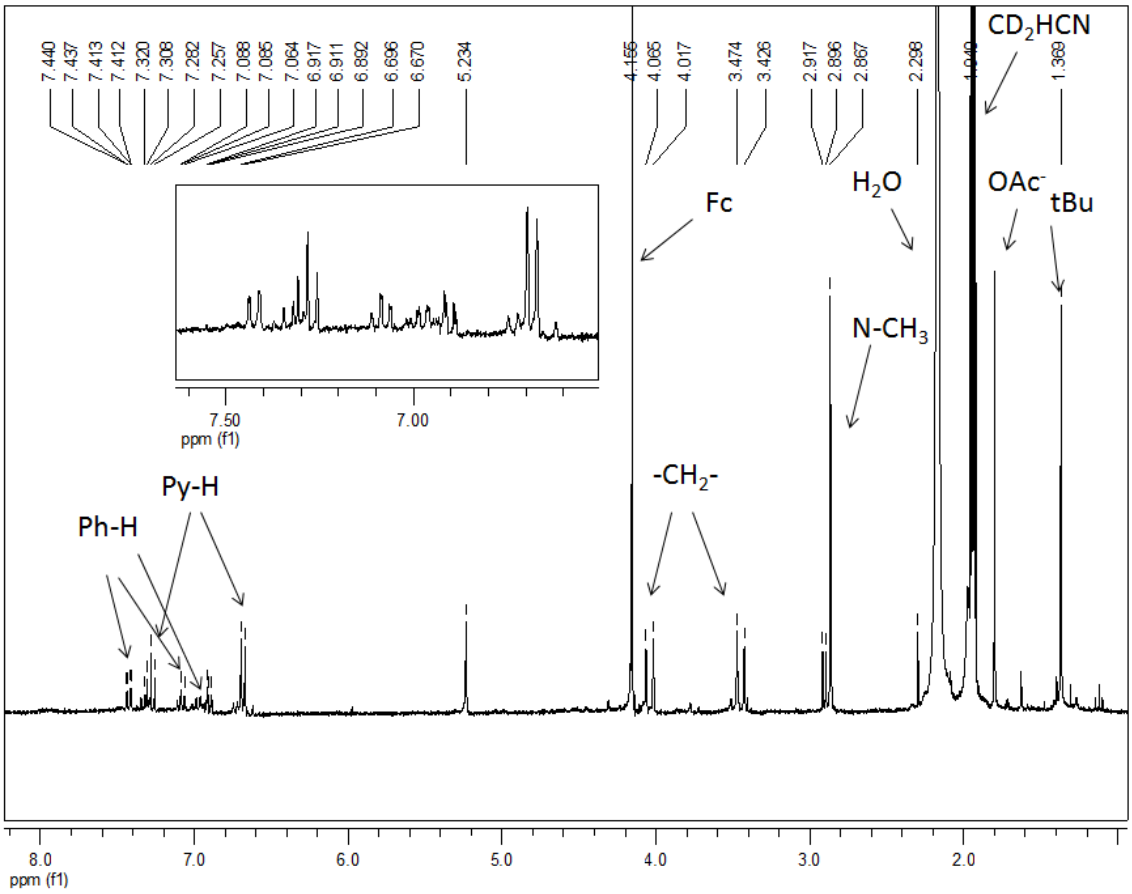

Figure S20. ^{1}H NMR spectrum of reaction mixture of in situ formed $\mathbf{1}^{+}$ with 2 equiv. of AgOAc in CD_3CN after 30 min.

KIE studies by ESI-MS Spectroscopy

The ESI-MS experiments were performed using a Bruker Maxis Q-TOF mass spectrometer with an electrospray ionization source. A 1:1 ratio of complex **1** (2.2 mg, 0.004 mmol) and complex **1-*d*$_5$** were mixed with $FcPF_6$ (2.8 mg, 0.008 mmol) in MeCN (1 mL) for 15 min, and this solution was measured by ESI-MS to confirm a 1:1 ratio of $\mathbf{1}^{+}$ and $\mathbf{1}^{+}$-d_5. Then AgOAc (1.6 mg, 0.009 mmol) was added to the reaction mixture. At 5 min, 15 min, 30 min and 50 min, ~1 μL aliquots were taken by pipet, diluted, and measured by ESI-MS immediately to monitor the progress of the reaction. The ESI-MS spectra show the existence of the following cationic intermediates during the reaction: $\mathbf{1}^{+}$ (m/z 542.1, calcd. 542.1), $\mathbf{1}^{+}$-$\boldsymbol{d_5}$ (m/z 547.2, calcd. 547.2), $\mathbf{2}^{+}$ (m/z 506.2, calcd. 506.2) and $\mathbf{2}^{+}$-$\boldsymbol{d_4}$ (m/z 510.2, calcd. 510.2). Note: the peaks at 548.2 and 511.2 corresponding to $\mathbf{1}^{+}$-d_6 and $\mathbf{2}^{+}$-d_5, the extra deuterium was on the methyl group or methylene group carried along from the neophyl chloride-d_5 starting material.

Over the monitored time course of the reaction, the ESI-MS peak intensity ratio of the cyclometalated products $\mathbf{2}^{+}$:$\mathbf{2}^{+}$-d_4 remained constant at ~1.3 (Figure S17). In addition, the

consumption of the starting material correlated well with the formation of cyclometalated product, as the ESI-MS peak intensity ratio of the starting material $\mathbf{1}^+$-d_5 :$\mathbf{1}^+$ was also ~1.3. Overall, a small kinetic isotopic effect (KIE = k_H/k_D = 1.28 ± 0.05) was measured for the C-H activation step.

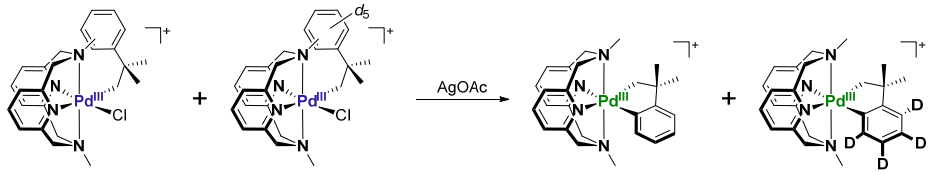

$\mathbf{1}^+$ $\mathbf{1}^+$-d_5 $\mathbf{2}^+$ $\mathbf{2}^+$-d_5

Time	$\mathbf{2}^+$	$\mathbf{2}^+$-d_4	$\mathbf{1}^+$	$\mathbf{1}^+$-d_5	$\mathbf{2}^+$ /$\mathbf{2}^+$-d_4	$\mathbf{1}^+$-d_5 /$\mathbf{1}^+$
1 min	0	0	0.943	1	Not detected	1.06
5 min	0.625	0.512	0.879	1	1.21	1.13
10 min	1	0.742	0.247	0.3	1.34	1.21
20 min	1	0.782	0.107	0.143	1.28	1.34
30 min	1	0.788	0.026	0.038	1.27	1.44
50 min	1	0.774	0.011	0.014	1.29	1.28
Average					**1.28±0.05**	**1.28±0.11**

$$\boldsymbol{KIE = k_H/k_D = 1.28\pm0.05}$$

Figure S21. Kinetic isotope data for the conversion from **1** to $\mathbf{1}^+$ and **1**-d_5 to $\mathbf{1}^+$-d_4 in the presence of AgOAc. Ratios at each time point determined by ESI-MS.

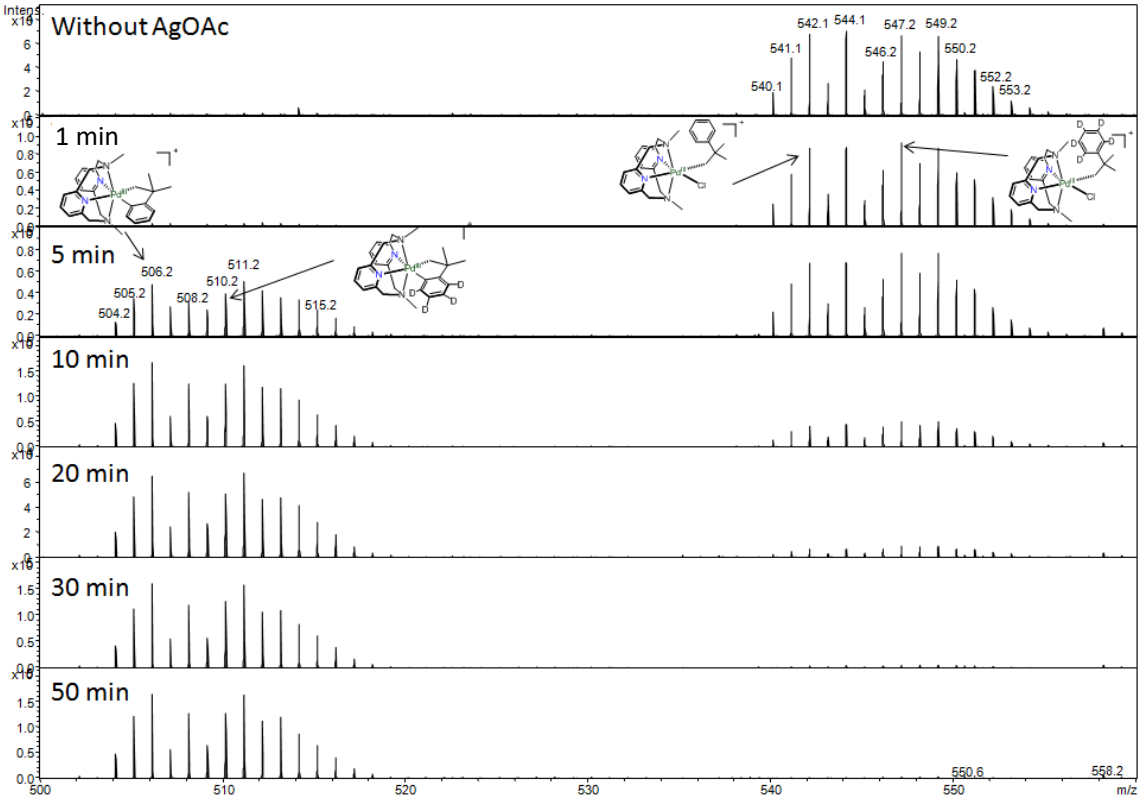

Figure S22. ESI-MS spectra for ~1:1 ratio of complex $\mathbf{1}^+$ and $\mathbf{1}^+$-$\boldsymbol{d_5}$ with AgOAc in MeCN at different time points.

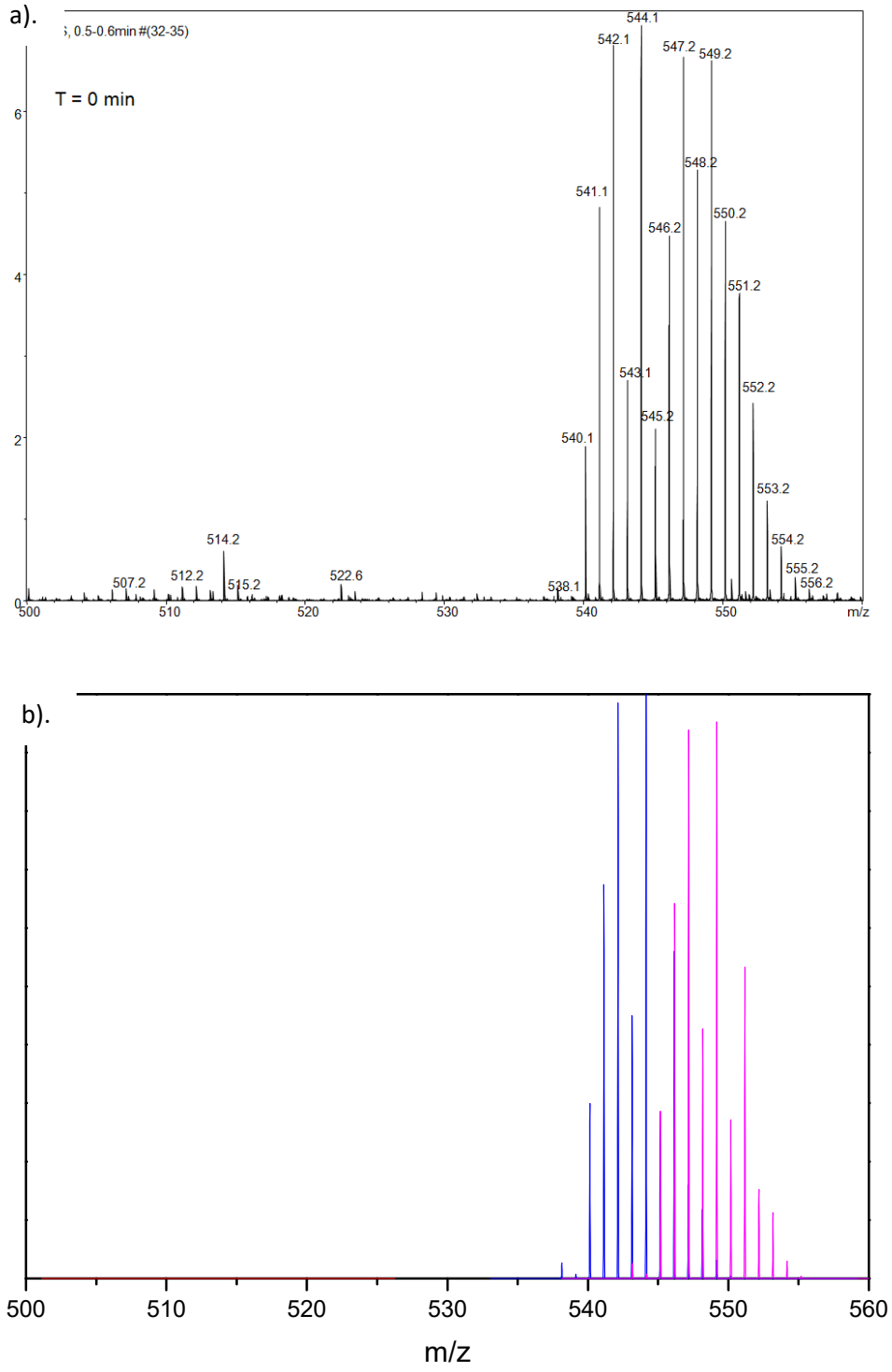

Figure S23. a). ESI-MS spectrum at the 0 min time point (before addition of AgOAc); b) Simulation of the isotopic pattern using a ~1:1 ratio of $\mathbf{1}^+$ and $\mathbf{1}^+$-d_5. Note: The variation of isotopic pattern of $\mathbf{1}^+$-d_5 is likely due to the incorporation of deuterium on the methylene group and methyl group of neophyl ligand.

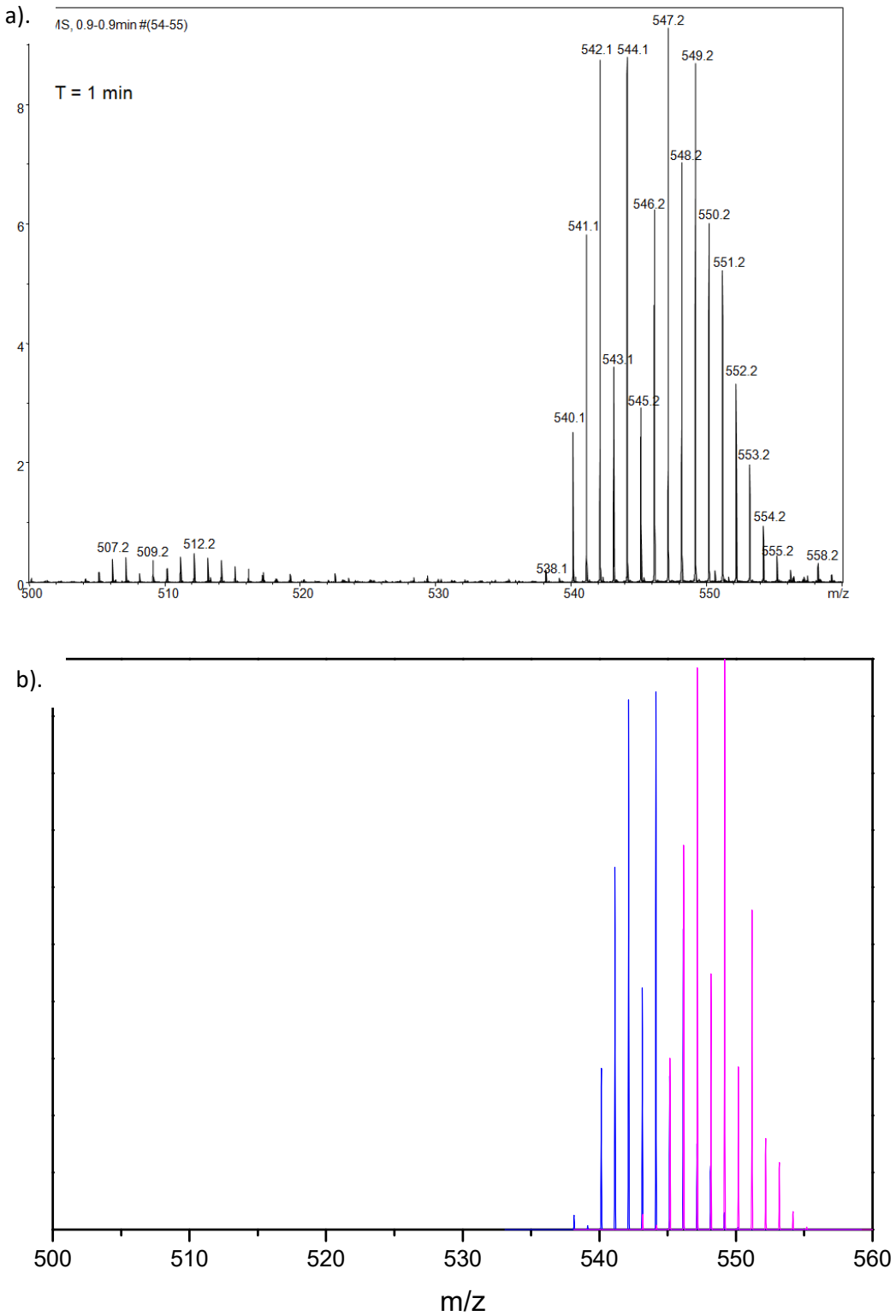

Figure S24. a). ESI-MS spectrum at the 1 min time point; b) Simulation of the isotopic pattern using a ~1:1 ratio of $\mathbf{1}^+$ and $\mathbf{1}^+$-d_5.

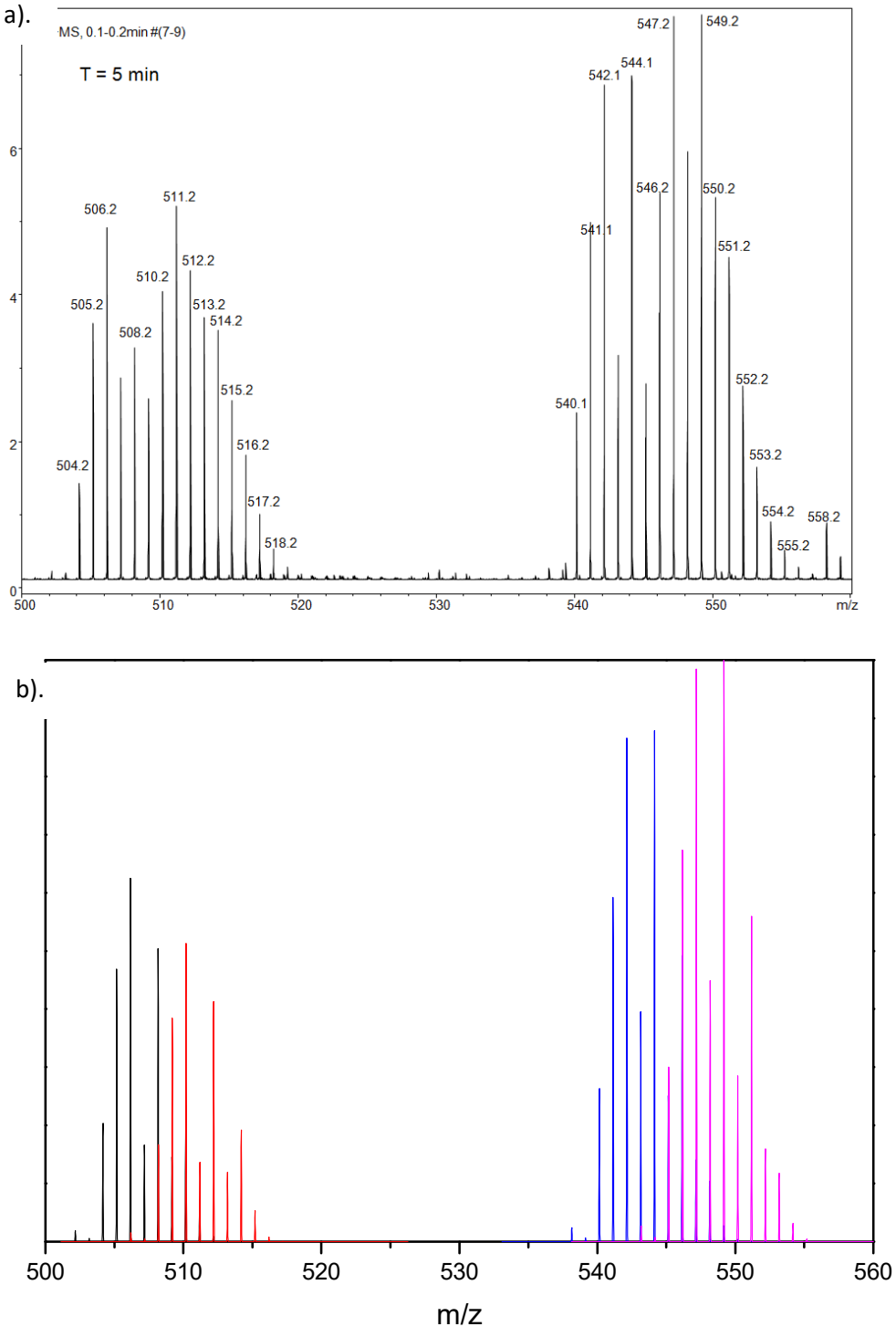

Figure S25. a). ESI-MS spectrum at the 5 min time point; b) Simulation of the isotopic pattern using a 0.6249:0.5123:0.8789:1 ratio of $\mathbf{2}^{+}$: $\mathbf{2}^{+}$-d_4 : $\mathbf{1}^{+}$: $\mathbf{1}^{+}$-d_5.

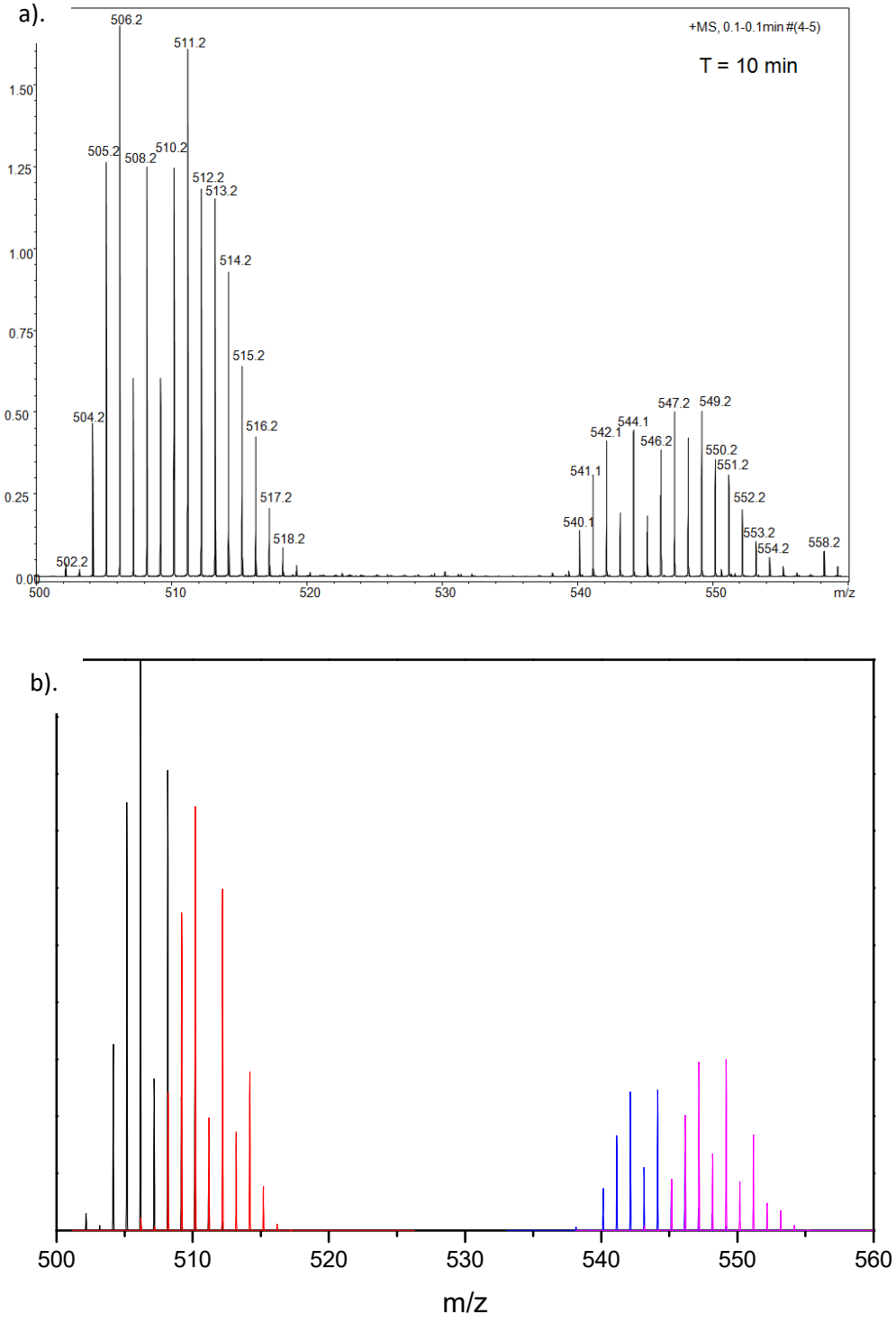

Figure S26. a). ESI-MS spectrum at the 10 min time point; b) Simulation of the isotopic pattern using a 1:0.7422:0.2465:0.2997 ratio of $\mathbf{2}^+$: $\mathbf{2}^+$-d_4 : $\mathbf{1}^+$: $\mathbf{1}^+$-d_5.

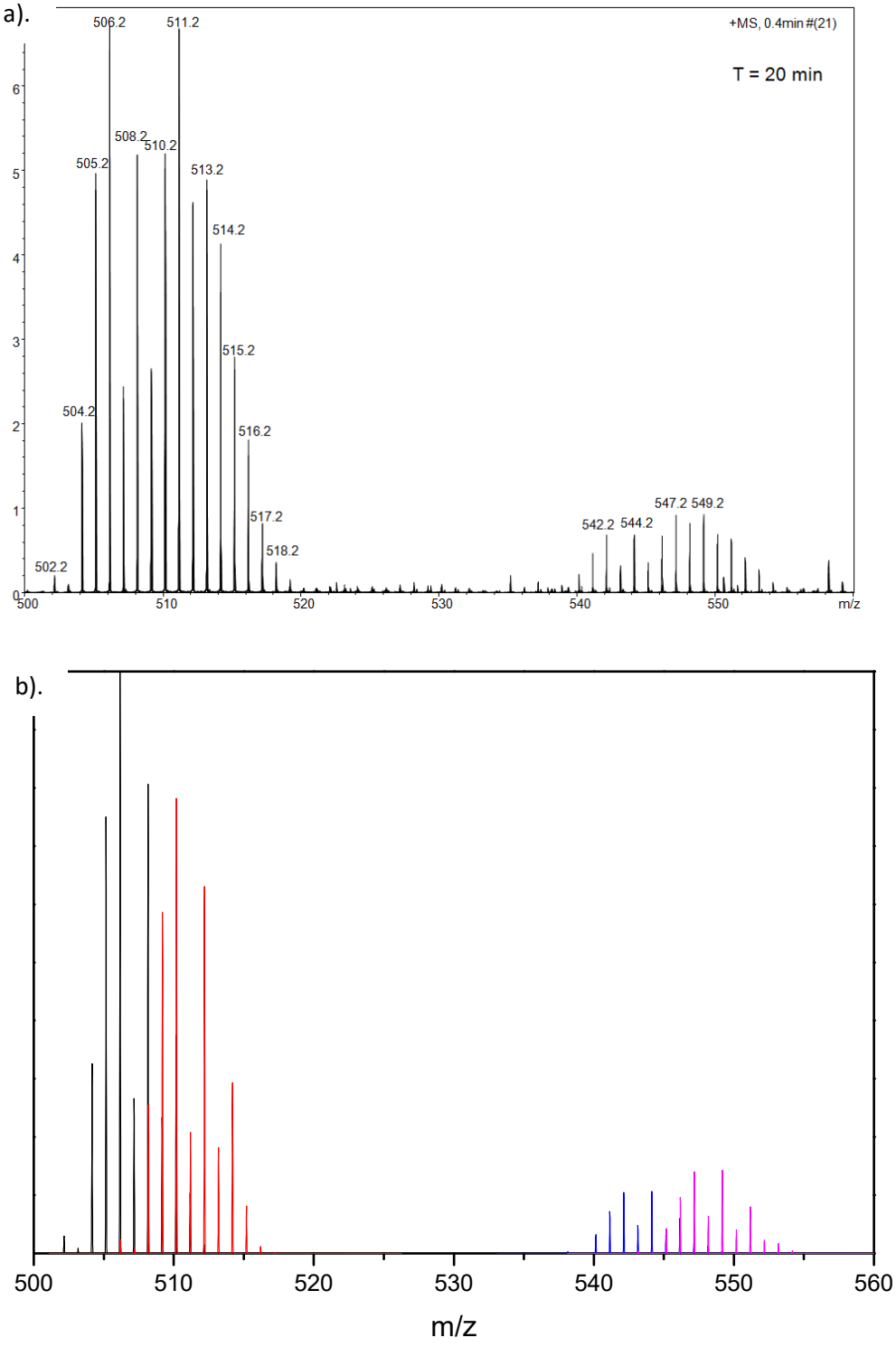

Figure S27 a). ESI-MS spectrum at the 20 min time point; b) Simulation of the isotopic pattern using a 1:0.7817:0.1065:0.1426 ratio of $\mathbf{2}^{+}$: $\mathbf{2}^{+}$-d_4 : $\mathbf{1}^{+}$: $\mathbf{1}^{+}$-d_5.

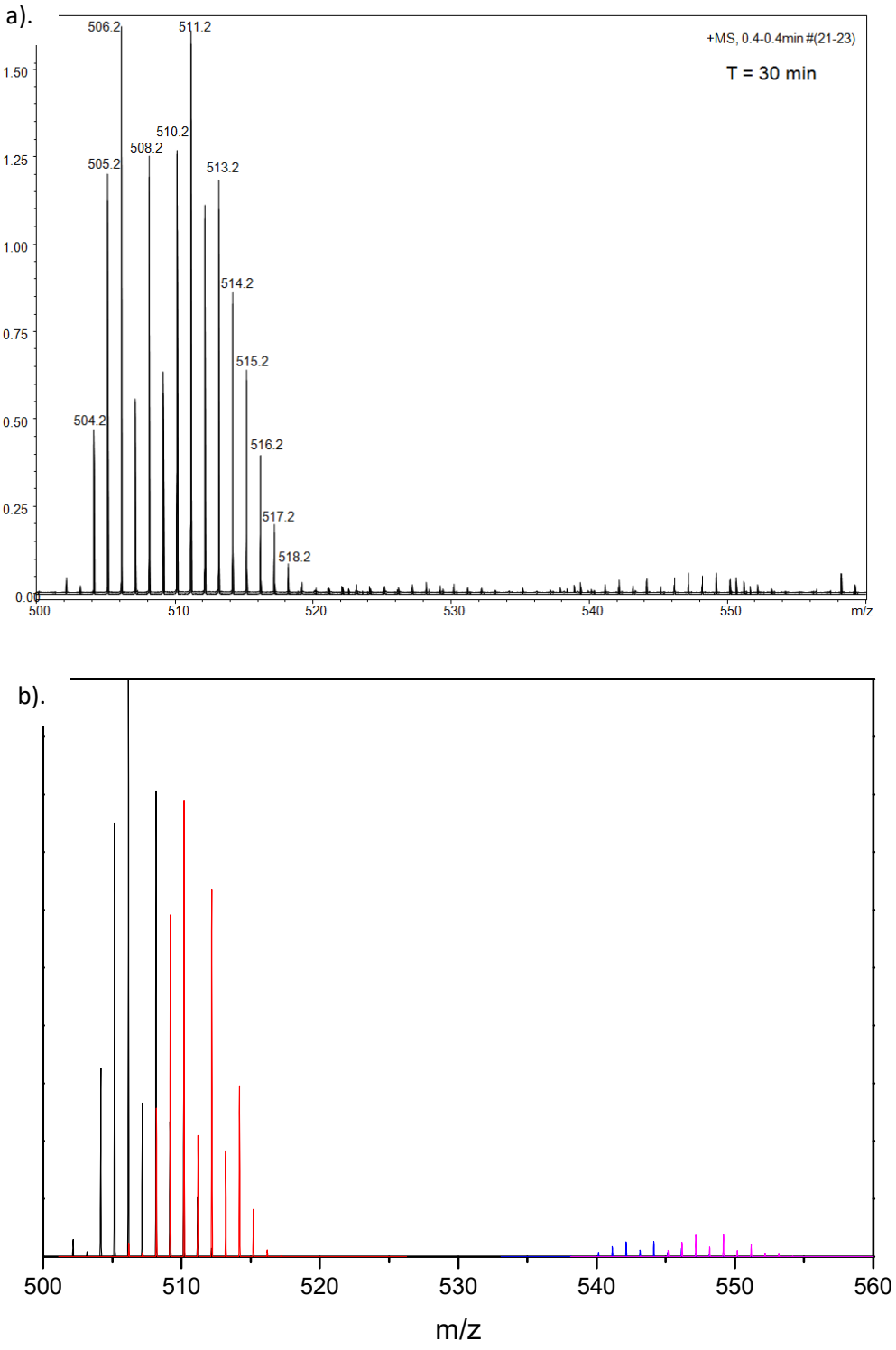

Figure S28. a). ESI-MS spectrum at the 30 min time point; b) Simulation of the isotopic pattern using a 1:0.7884:0.0263:0.0378 ratio of $\mathbf{2}^{+}$: $\mathbf{2}^{+}$-d_4 : $\mathbf{1}^{+}$: $\mathbf{1}^{+}$-d_5.

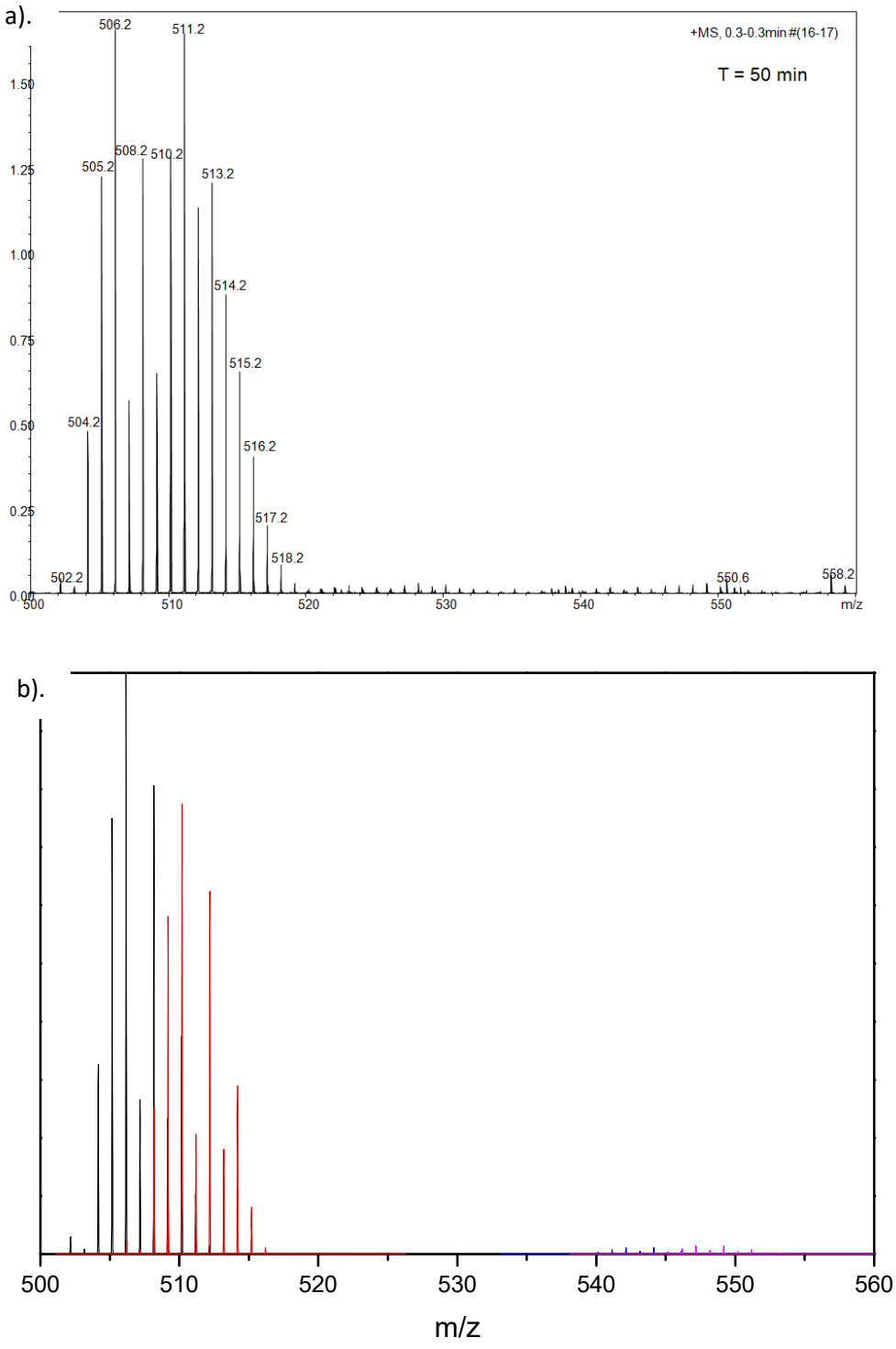

Figure S29. a). ESI-MS spectrum at the 50 min time point; b) Simulation of the isotopic pattern using a 1:0.7742:0.0111:0.0143 ratio of $\mathbf{2}^+$: $\mathbf{2}^+$-d_4 : $\mathbf{1}^+$: $\mathbf{1}^+$-d_5.

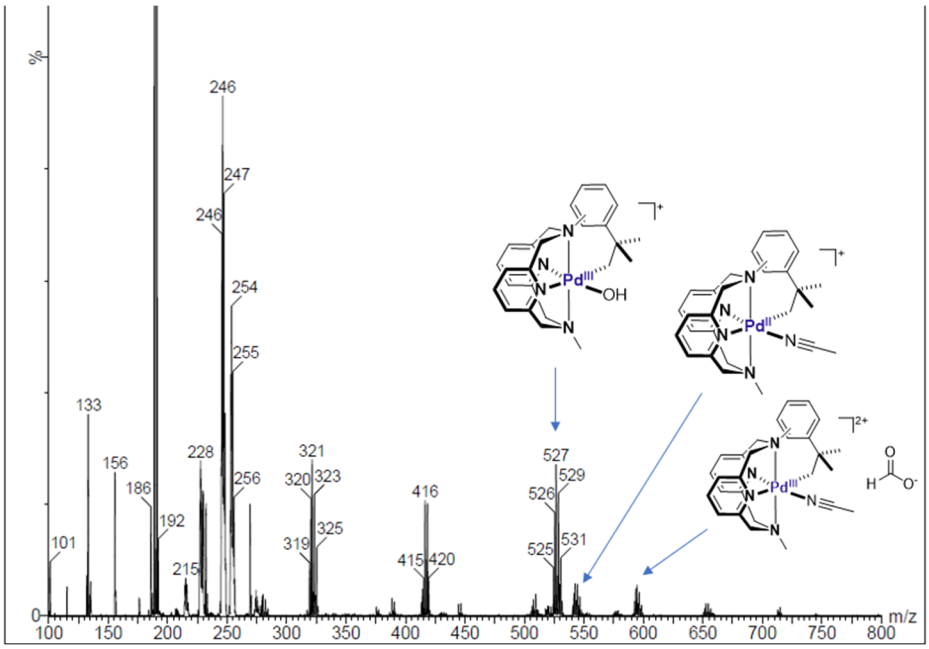

Figure S30. ESI-MS data for the reaction between $\mathbf{1}^{+}$ and 1 equiv. of $AgBF_4$ after 20 minutes in acetonitrile showing formation of acetonitrile adduct. The formate and hydroxide ions are present adventitiously in the ESI-MS instrument.

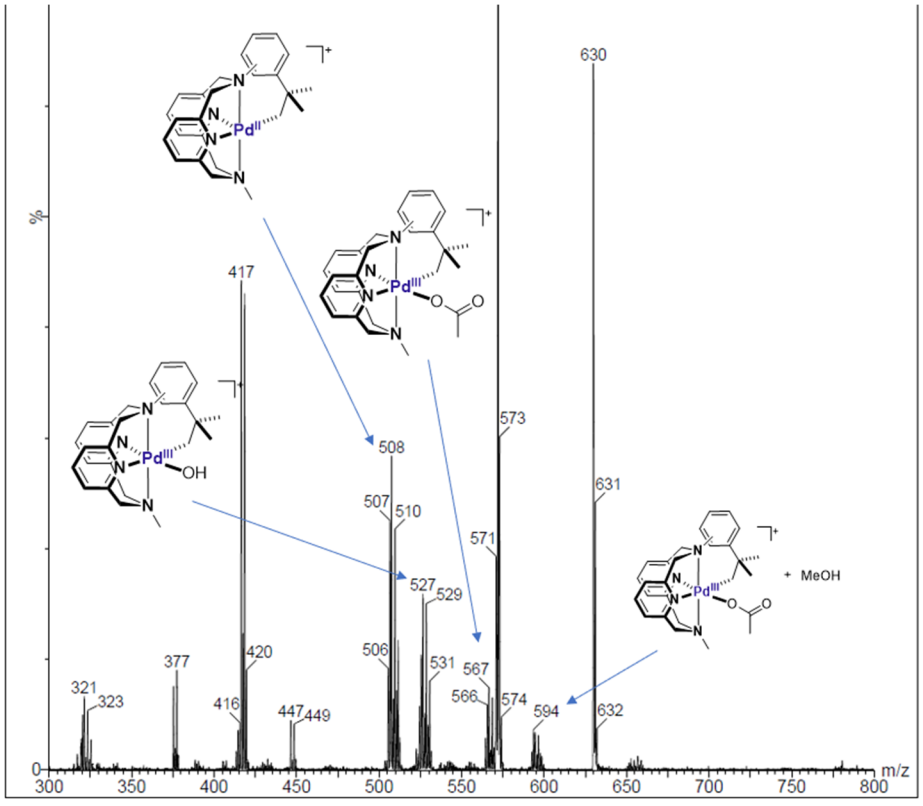

Figure S31. ESI-MS data for the reaction between in-situ generated **Int-A** and 1 equiv. of nBu_4OAc after 1 minute. The hydroxide ion and methanol are present adventitiously in the ESI-MS instrument.

IV. CV, UV-Vis, and EPR spectra

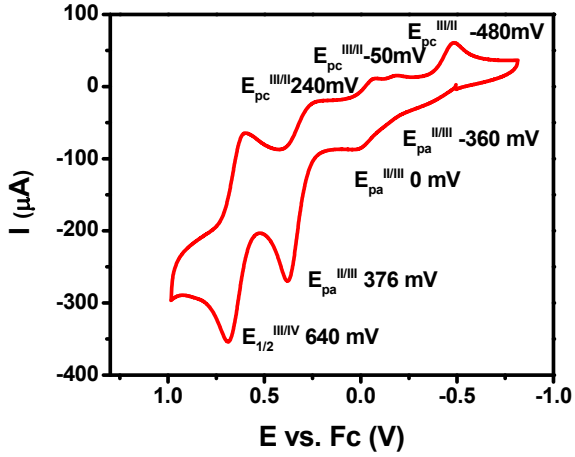

Figure S32. Cyclic voltammogram of complex **1** in 0.1 M Bu_4NClO_4/MeCN. Conditions: GCE, 100 mV/s. Note: Several anodic and cathodic waves corresponding to $Pd^{II/III}$ transitions are due to the oxidation and reduction of different conformers of the ligand in solution.

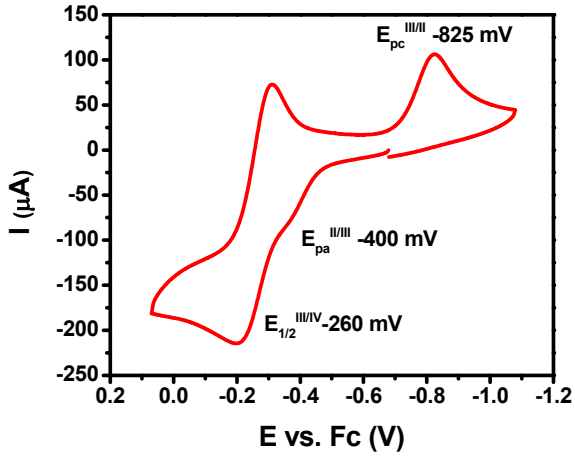

Figure S33. Cyclic voltammogram of complex **2** in 0.1 M Bu_4NClO_4/MeCN. Conditions: GCE, 100 mV/s.

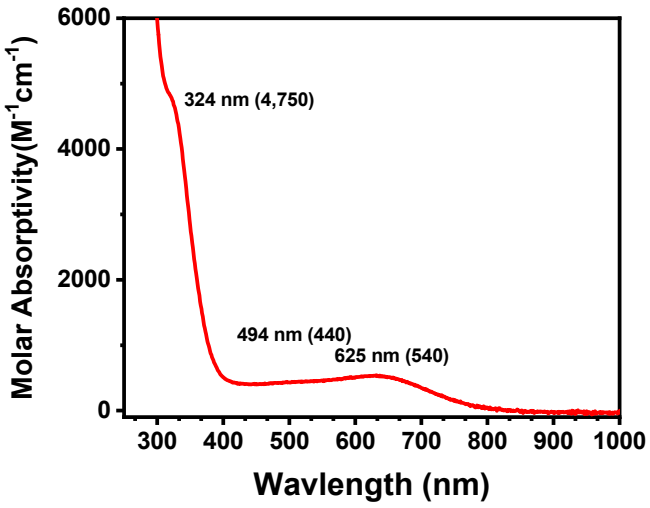

Figure S34. UV-vis spectrum of complex [**1**$^{+}$]ClO_4 in MeCN

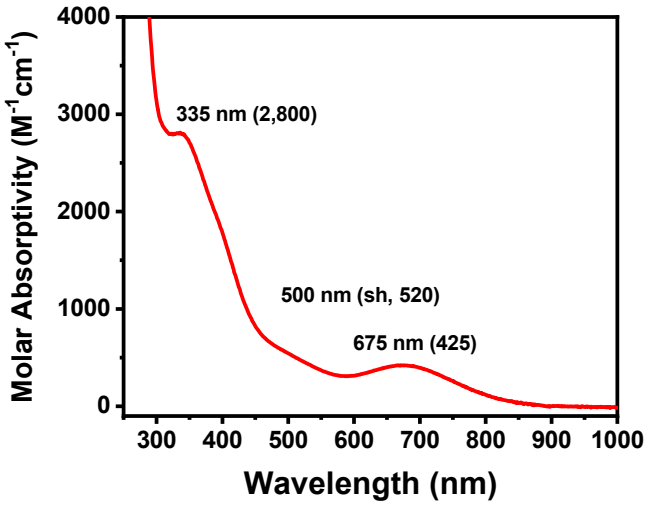

Figure S35. UV-vis spectrum of [**2**$^{+}$]ClO_4 in MeCN

EPR spectra

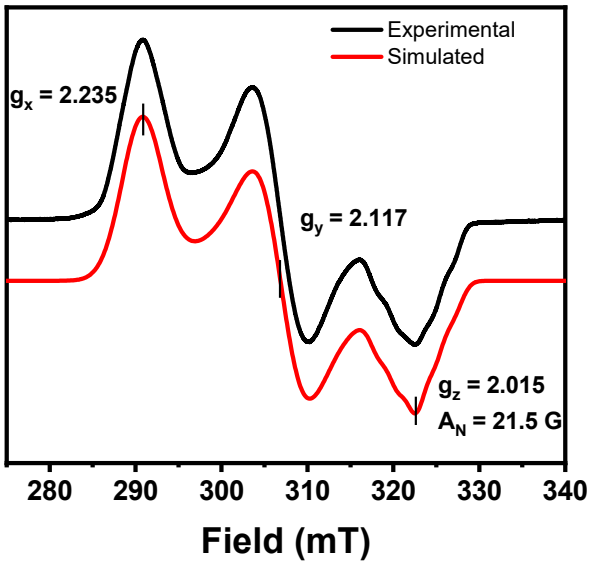

Figure S36. EPR spectrum of complex [**1**$^+$]ClO_4 in 3:1 PrCN/MeCN. $g_x = 2.235$, $g_y = 2.117$, $g_z = 2.015$ ($A_N = 21.5$ G).

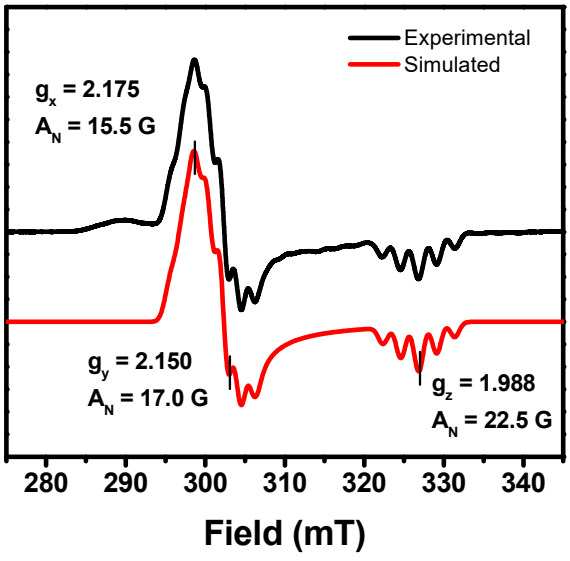

Figure S37. EPR spectrum of complex [**2**$^+$]ClO_4 in 3:1 PrCN/MeCN. $g_x = 2.175$ ($A_N = 15.5$ G), $g_y = 2.150$ ($A_N = 17.0$ G), $g_z = 1.988$ ($A_N = 22.5$ G).

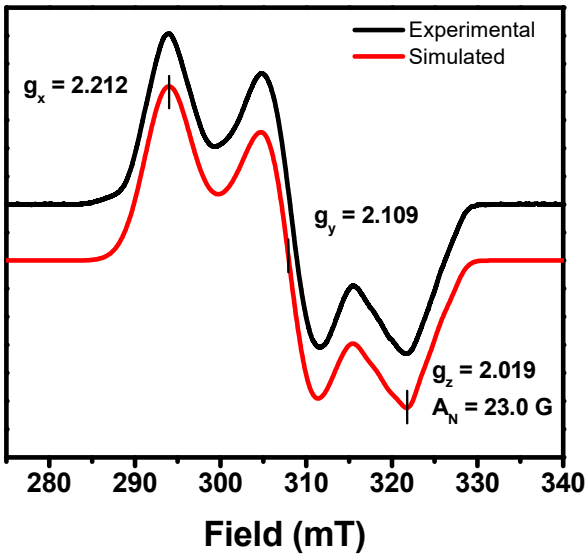

Figure S38. EPR spectrum of complex **Int-A** in 3:1 PrCN/MeCN. g_x = 2.212, g_y = 2.109, g_z = 2.019 (A_N = 23.0 G).

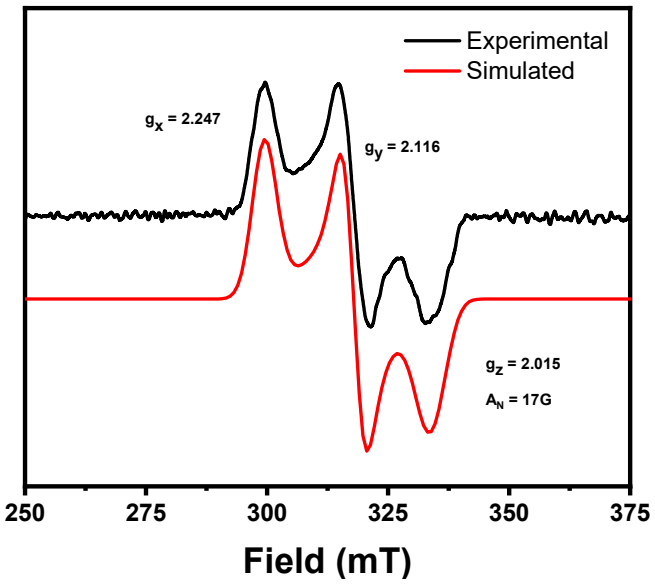

Figure S39. EPR spectrum of complex **Int-B** in 3:1 PrCN/MeCN.

V. Aerobic oxidation of complexes 1 and 2

In a UV-Vis cuvette equipped with a septum, complex **1** (2.0 mg, 0.004 mmol) was dissolve in O_2 saturated 5% H_2O/MeCN (2 mL) to make 1.84 mM solution, A peak at 675 nm corresponding to $\mathbf{2}^+$ grew slowly and reached its maximum point (0.532) in about 30 hours, and decayed slowly. Based on the extinction coefficient of $\mathbf{2}^+$ (425 $M^{-1}*cm^{-1}$), the yield is calculated as 68 %. The identity of $\mathbf{2}^+$ was also confirmed by EPR and ESI-Ms spectroscopy. The O_2 saturated solution was prepared by bubbling O_2 gas through the H_2O/MeCN solution for 10 minutes. Note: Addition of H_2O is to promote the formation of Pd^{III} species.[7]

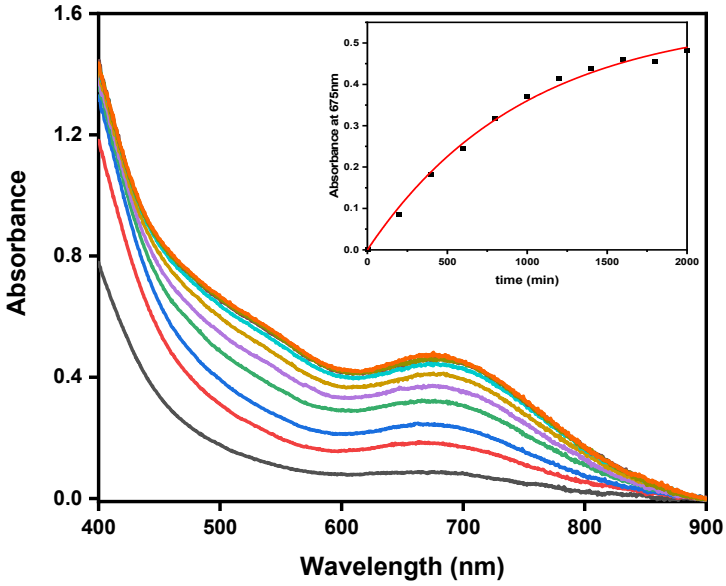

Figure S40. Formation of $\mathbf{2}^+$ during aerobic oxidation of complex **1** (1.84 mM) in O_2 saturated 5% H_2O/MeCN followed by UV-vis spectroscopy (Δt = 200 min, t_{max} = 2000 min). Inset: plot of the concentration of $\mathbf{2}^+$ monitored at 675 nm and first-order fitting (red line, k = 0.00103 min^{-1}, R^2 = 0.995).

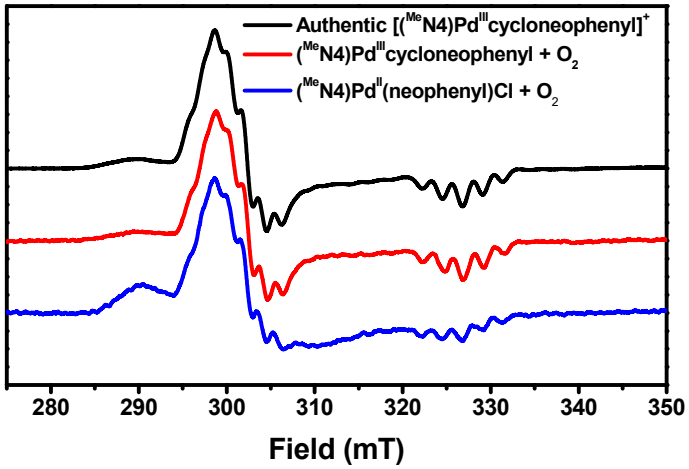

Figure S41. EPR spectrum of ($\mathbf{2}^{+}$) in 3:1 PrCN/MeCN. $g_x = 2.175$ ($A_N = 15.5$ G), $g_y = 2.150$ ($A_N = 17.0$ G), $g_z = 1.988$ ($A_N = 22.5$ G). Black: authentic [$\mathbf{2}^{+}$]ClO_4. Red: reaction mixture of complex **2** with O_2 in Blue: Reaction mixture of **1** with O_2.

VI. ORTEP and space-filling models of [1], [1^{+}], [2], [2^{+}] and [2^{2+}]

Table S4. ORTEP diagrams and space filling models for **[1]**, **[1^{+}]**, **[2]**, **[2^{+}]** and **[2^{2+}]**

(^{Me}N4)Pd^{II}(neophyl)Cl [**1**] 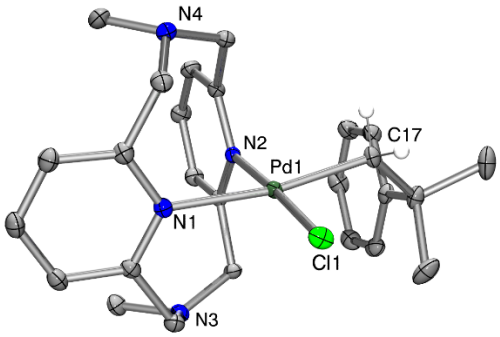	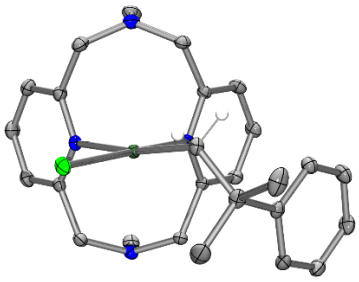	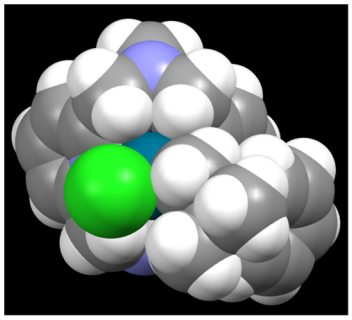
[(^{Me}N4)Pd^{III}(neophyl)Cl]$^{+}$ [**1**$^{+}$] 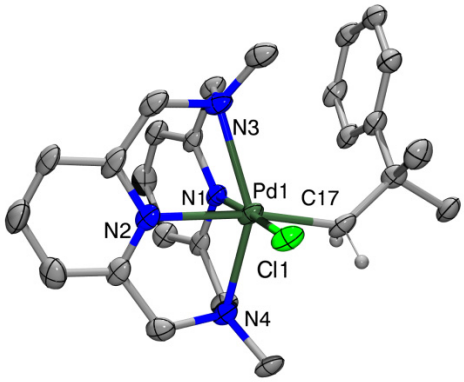	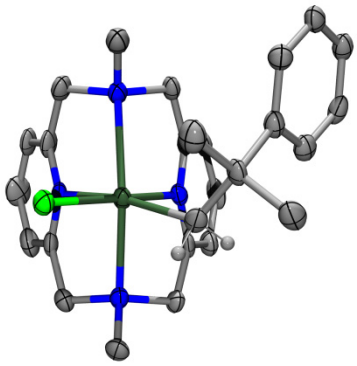	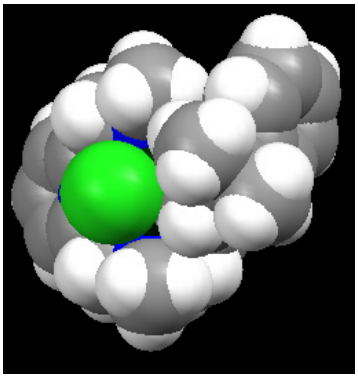
(^{Me}N4)Pd^{III}(cycloneophyl) (**2**) 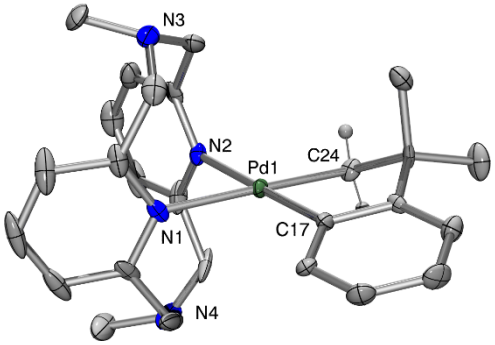	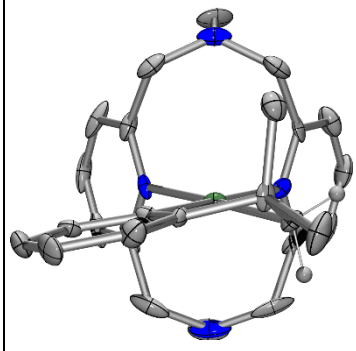	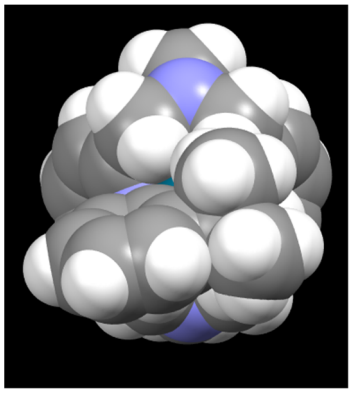

[(^{Me}N4)Pd^{III}(cycloneophyl)]$^+$ (**2**$^+$) 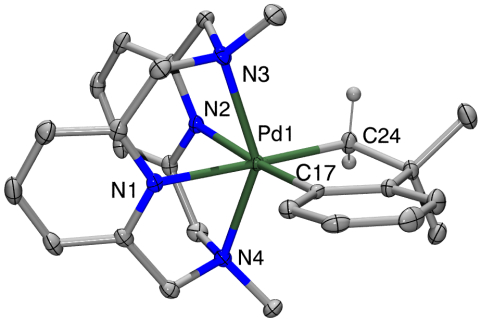	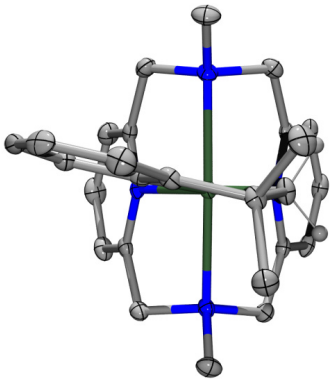	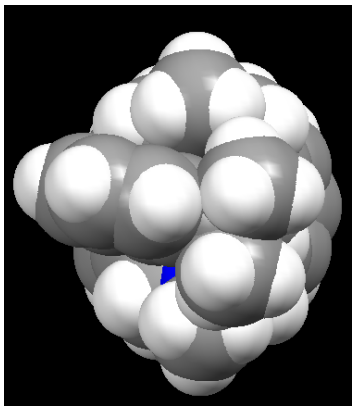
[(^{Me}N4)Pd^{IV}(cycloneophyl)]$^+$ (**2**$^{2+}$) 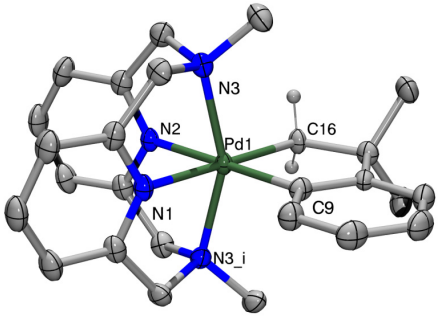	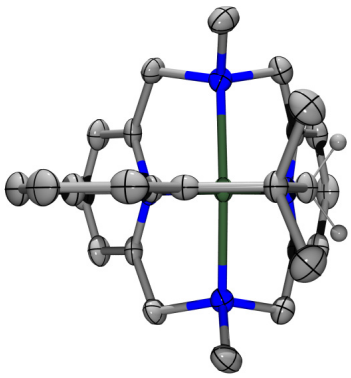	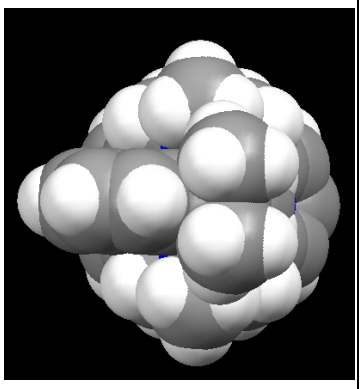

VII. X-ray crystallographic data of 1, 2, $[2^+]PF_6$, and $[2^{2+}](ClO_4)_2$

General information: Crystals of x-ray diffraction quality were obtained by slow ether vapor diffusion or layering into the corresponding acetonitrile solution of **1**, **2**, **3**, **4**. Suitable crystals of appropriate dimensions were mounted on Mitgen loops in random orientations. Preliminary examination and data collection were performed using a Bruker Kappa Apex-II Charge Coupled Device (CCD) Detector system single crystal X-Ray diffractometer equipped with an Oxford Cryostream LT device. Data were collected using graphite monochromated Mo Kα radiation (λ= 0.71073 Å) from a fine focus sealed tube X-Ray source. Preliminary unit cell constants were determined with a set of 36 narrow frame scans. Typical data sets consist of a combination of ϖ and ϕ scan frames with typical scan width of 0.5° and counting time of 15-30 seconds/frame at a crystal to detector distance of ~4.0 cm. The collected frames were integrated using an orientation matrix determined from the narrow frame scans. Apex II and SAINT software packages (*Bruker Analytical X-Ray, Madison, WI, 2008*) were used for data collection and data integration. Analysis of the integrated data did not show any decay. Final cell constants were determined by global refinement of reflections from the complete data set. Data were corrected for systematic errors using SADABS (*Bruker Analytical X-Ray, Madison, WI, 2008*) based on the Laue symmetry using equivalent reflections.

Structure solutions and refinement were carried out using the SHELXTL- PLUS software package. The structures were refined with full matrix least-squares refinement by minimizing $\Sigma w(F_o^2-F_c^2)^2$. All non-hydrogen atoms were refined anisotropically to convergence. Typically, H atoms are added at the calculated positions in the final refinement cycles.

Acknowledgement: Funding from the National Science Foundation (MRI, CHE-0420497) for the purchase of the Apex II diffractometer is acknowledged.

X-ray structure determinations of [1], $[1^+]$, [2], $[2^+]$, and $[2^{2+}]$

Table S5. Crystal data and structure refinement for 1.

Identification code	MeN4PdNeophylCl
Empirical formula	$C_{26}H_{33}ClN_4Pd$
Formula weight	543.41
Temperature/K	100.0
Crystal system	monoclinic
Space group	$P2_1/c$
a/Å	8.7777(2)

b/Å	30.6361(6)
c/Å	9.7205(2)
α/°	90
β/°	113.69
γ/°	90
Volume/Å^3	2393.64(9)
Z	4
ρ_{calc}g/cm^3	1.508
μ/mm^{-1}	0.908
F(000)	1120.0
Crystal size/mm^3	0.225 × 0.124 × 0.088
Radiation	MoKα (λ = 0.71073)
2Θ range for data collection/°	4.766 to 56.59
Index ranges	-11 ≤ h ≤ 11, -40 ≤ k ≤ 40, -12 ≤ l ≤ 12
Reflections collected	81975
Independent reflections	5949 [R_{int} = 0.0249, R_{sigma} = 0.0103]
Data/restraints/parameters	5949/0/293
Goodness-of-fit on F^2	1.100
Final R indexes [I>=2σ (I)]	R_1 = 0.0178, wR_2 = 0.0431
Final R indexes [all data]	R_1 = 0.0185, wR_2 = 0.0435
Largest diff. peak/hole / e Å^{-3}	0.39/-0.50

Table S6. Fractional Atomic Coordinates (×10^4) and Equivalent Isotropic Displacement Parameters (Å^2×10^3) for 1. U_{eq} is defined as 1/3 of of the trace of the orthogonalised U_{IJ} tensor.

Atom	x	y	z	U(eq)
Pd1	4327.2(2)	3843.7(2)	3405.9(2)	11.22(3)
Cl1	7111.9(4)	4025.7(2)	4731.1(4)	17.27(6)
N1	3651.3(13)	4480.2(3)	2341.7(12)	13.8(2)
N2	1841.4(13)	3717.9(3)	2239.1(11)	11.58(19)
N4	2860.1(15)	3845.7(4)	-657.6(13)	17.5(2)
N3	1523.8(13)	4525.4(3)	4432.1(12)	15.1(2)
C1	3625.1(16)	4535.0(4)	951.6(14)	15.7(2)
C17	4870.8(15)	3208.4(4)	4069.0(14)	14.1(2)
C13	1278.1(16)	3550.7(4)	833.0(13)	13.8(2)
C4	2643.3(17)	5210.0(4)	2267.1(15)	18.3(2)
C8	1382.3(15)	4049.1(4)	4375.2(13)	13.6(2)
C12	-404.5(16)	3463.7(4)	33.7(14)	18.1(2)
C2	3116.0(17)	4927.7(4)	183.1(15)	19.0(3)
C5	3143.2(15)	4808.4(4)	2982.4(14)	14.4(2)

C9	747.0(15)	3830.3(4)	2841.8(14)	12.6(2)
C3	2622.2(17)	5268.9(4)	847.2(16)	20.5(3)
C26	1913.1(17)	3105.3(4)	5910.7(15)	18.2(2)
C16	4150.5(16)	4156.4(4)	228.6(15)	17.6(2)
C21	2691.1(16)	2953.6(4)	5001.1(14)	15.1(2)
C14	2504.7(16)	3473.6(4)	114.9(14)	15.8(2)
C20	5348.9(18)	2551.9(5)	5683.5(18)	26.2(3)
C18	4549.4(16)	3013.0(4)	5386.4(15)	17.4(2)
C24	-735.0(17)	2815.8(5)	4217.0(17)	21.5(3)
C6	3065.5(16)	4724.4(4)	4490.6(14)	15.6(2)
C10	-945.2(16)	3748.4(4)	2076.3(15)	16.2(2)
C25	215.6(18)	3041.5(4)	5510.4(16)	20.7(3)
C22	1705.7(16)	2725.6(4)	3691.9(15)	16.8(2)
C23	25.0(17)	2658.3(4)	3307.4(16)	20.1(3)
C11	-1529.3(16)	3558.8(4)	664.4(15)	18.9(3)
C7	18.6(17)	4753.3(4)	3460.3(15)	19.2(3)
C15	1398.9(19)	4050.2(5)	-1796.0(15)	22.4(3)
C19	5427.5(19)	3288.7(5)	6803.6(15)	26.4(3)

Table S7. Bond lengths for 1.

Atom	Atom	Length/Å	Atom	Atom	Length/Å
Pd1	Cl1	2.3268(3)	C13	C14	1.5187(17)
Pd1	N1	2.1750(10)	C4	C5	1.3946(17)
Pd1	N2	2.0511(10)	C4	C3	1.3846(19)
Pd1	C17	2.0454(12)	C8	C9	1.5212(16)
N1	C1	1.3526(16)	C12	C11	1.3863(19)
N1	C5	1.3495(16)	C2	C3	1.3865(19)
N2	C13	1.3535(15)	C5	C6	1.5167(17)
N2	C9	1.3553(15)	C9	C10	1.3909(17)
N4	C16	1.4653(17)	C26	C21	1.3963(18)
N4	C14	1.4660(16)	C26	C25	1.3942(19)
N4	C15	1.4566(17)	C21	C18	1.5307(17)
N3	C8	1.4635(16)	C21	C22	1.4039(18)
N3	C6	1.4643(16)	C20	C18	1.5521(19)
N3	C7	1.4569(16)	C18	C19	1.5335(19)
C1	C2	1.3917(18)	C24	C25	1.383(2)
C1	C16	1.5207(18)	C24	C23	1.3906(19)
C17	C18	1.5389(17)	C10	C11	1.3851(18)
C13	C12	1.3906(18)	C22	C23	1.3840(18)

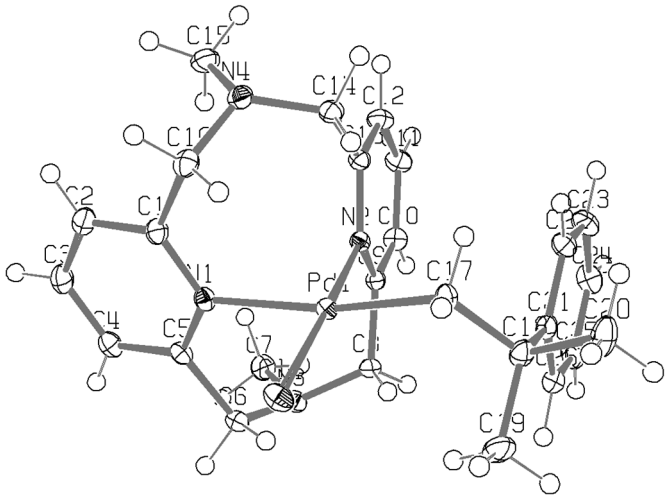

Figure S42. Projection view of [**1**] with 50% thermal ellipsoids.

Table S8. Crystal data and structure refinement for **[1$^+$]**.

Identification code	l13213/lt/smart/FT-080713	
Empirical formula	C_{34} H_{51} Cl_3 Li N_4 O_{11} Pd	
Formula weight	911.47	
Temperature	100(2) K	
Wavelength	0.71073 Å	
Crystal system	Monoclinic	
Space group	P 2_1/c	
Unit cell dimensions	a = 14.0733(11) Å	α = 90°.
	b = 18.7386(15) Å	β = 109.564(5)°.
	c = 15.8690(12) Å	γ = 90°.
Volume	3943.3(5) Å^3	
Z	4	
Density (calculated)	1.535 Mg/m^3	
Absorption coefficient	0.736 mm^{-1}	
F(000)	1884	
Crystal size	0.322 x 0.249 x 0.054 mm^3	
Theta range for data collection	1.742 to 25.403°.	
Index ranges	-16⩽h⩽16, -22⩽k⩽15, -19⩽l⩽19	
Reflections collected	45191	

Independent reflections	7230 [R(int) = 0.1157]
Completeness to theta = 25.242°	100.0 %
Absorption correction	Semi-empirical from equivalents
Max. and min. transmission	0.9281 and 0.7625
Refinement method	Full-matrix least-squares on F^2
Data / restraints / parameters	7230 / 333 / 502
Goodness-of-fit on F^2	1.011
Final R indices [I>2sigma(I)]	R1 = 0.0578, wR2 = 0.1236
R indices (all data)	R1 = 0.1178, wR2 = 0.1533
Extinction coefficient	n/a
Largest diff. peak and hole	1.007 and -0.921 e.Å^{-3}

Table S9. Atomic coordinates (x 10^4) and equivalent isotropic displacement parameters (Å^{2}x 10^3) for **[1$^+$]**. U(eq) is defined as one third of the trace of the orthogonalized U^{ij} tensor.

	x	y	z	U(eq)
Pd(1)	9902(1)	6276(1)	1678(1)	25(1)
Cl(1)	11003(1)	5469(1)	1322(1)	31(1)
N(1)	8890(4)	6927(3)	1996(3)	25(1)
N(2)	8888(4)	5489(3)	1895(3)	27(1)
N(3)	10412(4)	6141(3)	3268(3)	30(1)
N(4)	8597(4)	6296(3)	335(3)	27(1)
C(1)	8019(5)	7082(3)	1332(4)	27(2)
C(2)	7195(5)	7346(3)	1517(4)	32(2)
C(3)	7252(5)	7412(3)	2404(5)	38(2)

C(4)	8125(5)	7203(3)	3077(4)	30(2)
C(5)	8933(5)	6965(3)	2864(4)	26(2)
C(6)	9918(5)	6760(3)	3540(4)	28(2)
C(7)	9980(5)	5451(3)	3417(4)	34(2)
C(8)	8964(6)	5298(3)	2726(4)	36(1)
C(9)	8180(6)	4980(3)	2919(5)	36(1)
C(10)	7304(6)	4850(4)	2229(5)	49(2)
C(11)	7201(6)	5069(3)	1358(5)	40(2)
C(12)	8020(5)	5392(3)	1222(4)	30(2)
C(13)	8019(5)	5626(3)	319(4)	31(2)
C(14)	8037(5)	6955(3)	398(4)	27(2)
C(15)	11502(5)	6133(3)	3799(4)	37(2)
C(16)	8882(5)	6326(3)	-481(4)	32(2)
C(17)	10593(5)	7123(3)	1268(4)	30(2)
C(18)	11529(5)	7521(3)	1824(4)	27(2)
C(19)	11697(5)	8104(3)	1203(4)	35(2)
C(20)	12449(5)	7021(4)	2089(4)	37(2)
C(21)	11384(5)	7919(3)	2623(4)	28(2)
C(22)	12130(5)	7933(3)	3465(4)	30(2)
C(23)	12002(5)	8319(3)	4165(4)	32(2)
C(24)	11132(5)	8709(3)	4029(4)	33(2)
C(25)	10383(5)	8713(3)	3196(4)	33(2)
C(26)	10517(5)	8321(3)	2507(4)	31(2)
Cl(2)	8021(1)	9050(1)	212(1)	38(1)
O(1)	8185(10)	9033(6)	1166(3)	49(2)
O(2)	7294(4)	8515(3)	-217(4)	47(2)
O(3)	7650(6)	9741(2)	-99(4)	80(2)
O(4)	8964(4)	8863(4)	113(4)	78(2)
O(1')	8310(150)	9000(80)	1169(8)	49(2)
O(2')	7250(50)	8790(30)	-580(30)	47(2)
O(3')	8510(60)	9660(30)	-10(40)	80(2)
O(4')	7740(50)	9000(60)	-748(8)	78(2)
Cl(3)	5234(1)	8449(1)	3890(1)	45(1)
O(5)	6012(3)	8597(2)	3489(3)	40(1)
O(6)	4270(4)	8509(4)	3212(4)	68(2)
O(7)	5411(5)	7741(3)	4255(5)	70(2)

O(8)	5373(7)	8960(4)	4594(5)	92(3)
O(6')	4500(20)	9004(15)	3560(20)	68(2)
O(7')	5740(30)	8520(20)	4839(8)	70(2)
O(8')	4860(30)	7782(13)	3450(30)	92(3)
Li(1)	5973(9)	9247(7)	2487(8)	43(2)
O(9)	5305(4)	10104(3)	2688(4)	59(2)
O(10)	5272(4)	8787(3)	1378(3)	58(2)
O(11)	7258(4)	9484(3)	2387(3)	48(1)
C(27)	5655(8)	10525(4)	3512(6)	73(3)
C(28)	5104(7)	11221(5)	3309(6)	71(2)
C(29)	4653(10)	11232(6)	2322(7)	104(4)
C(30)	4863(10)	10564(5)	1963(6)	105(4)
C(31)	4382(7)	8365(6)	1257(6)	88(2)
C(32)	3965(8)	8165(6)	356(6)	88(2)
C(33)	4328(7)	8728(5)	-144(5)	67(2)
C(34)	5312(6)	8970(5)	515(5)	54(2)

Table S10. Bond lengths [Å] for **[1$^+$]**.

Pd(1)-N(1)	2.061(5)	N(3)-C(6)	1.488(7)
Pd(1)-C(17)	2.076(6)	N(4)-C(16)	1.479(7)
Pd(1)-N(2)	2.158(5)	N(4)-C(14)	1.486(7)
Pd(1)-N(4)	2.301(5)	N(4)-C(13)	1.492(8)
Pd(1)-Cl(1)	2.3667(16)	C(1)-C(2)	1.380(8)
Pd(1)-N(3)	2.394(5)	C(1)-C(14)	1.509(8)
N(1)-C(1)	1.353(8)	C(2)-C(3)	1.388(9)
N(1)-C(5)	1.361(7)	C(2)-H(2)	0.9500
N(2)-C(8)	1.336(7)	C(3)-C(4)	1.387(9)
N(2)-C(12)	1.338(8)	C(3)-H(3)	0.9500
N(3)-C(7)	1.481(8)	C(4)-C(5)	1.365(8)
N(3)-C(15)	1.483(8)	C(4)-H(4)	0.9500

C(5)-C(6)	1.492(9)	C(21)-C(26)	1.393(9)
C(6)-H(6A)	0.9900	C(21)-C(22)	1.396(9)
C(6)-H(6B)	0.9900	C(22)-C(23)	1.387(8)
C(7)-C(8)	1.509(9)	C(22)-H(22)	0.9500
C(7)-H(7A)	0.9900	C(23)-C(24)	1.380(9)
C(7)-H(7B)	0.9900	C(23)-H(23)	0.9500
C(8)-C(9)	1.377(9)	C(24)-C(25)	1.388(9)
C(9)-C(10)	1.370(10)	C(24)-H(24)	0.9500
C(9)-H(9)	0.9500	C(25)-C(26)	1.382(8)
C(10)-C(11)	1.402(9)	C(25)-H(25)	0.9500
C(10)-H(10)	0.9500	C(26)-H(26)	0.9500
C(11)-C(12)	1.382(9)	Cl(2)-O(3)	1.421(5)
C(11)-H(11)	0.9500	Cl(2)-O(4)	1.431(5)
C(12)-C(13)	1.497(8)	Cl(2)-O(2)	1.432(4)
C(13)-H(13A)	0.9900	Cl(2)-O(2')	1.437(8)
C(13)-H(13B)	0.9900	Cl(2)-O(1')	1.438(8)
C(14)-H(14A)	0.9900	Cl(2)-O(3')	1.440(8)
C(14)-H(14B)	0.9900	Cl(2)-O(4')	1.443(8)
C(15)-H(15A)	0.9800	Cl(2)-O(1)	1.454(4)
C(15)-H(15B)	0.9800	Cl(3)-O(6)	1.426(5)
C(15)-H(15C)	0.9800	Cl(3)-O(7)	1.434(5)
C(16)-H(16A)	0.9800	Cl(3)-O(8)	1.434(5)
C(16)-H(16B)	0.9800	Cl(3)-O(6')	1.439(8)
C(16)-H(16C)	0.9800	Cl(3)-O(7')	1.440(8)
C(17)-C(18)	1.514(9)	Cl(3)-O(8')	1.442(8)
C(17)-H(17A)	0.9900	Cl(3)-O(5)	1.466(4)
C(17)-H(17B)	0.9900	O(5)-Li(1)	1.989(13)
C(18)-C(20)	1.538(9)	Li(1)-O(10)	1.910(13)
C(18)-C(21)	1.541(8)	Li(1)-O(11)	1.920(13)
C(18)-C(19)	1.542(8)	Li(1)-O(9)	1.940(13)
C(19)-H(19A)	0.9800	O(9)-C(30)	1.405(10)
C(19)-H(19B)	0.9800	O(9)-C(27)	1.464(10)
C(19)-H(19C)	0.9800	O(10)-C(34)	1.431(8)
C(20)-H(20A)	0.9800	O(10)-C(31)	1.438(9)
C(20)-H(20B)	0.9800	O(11)-H(11A)	0.8710
C(20)-H(20C)	0.9800	O(11)-H(11B)	0.8713

C(27)-C(28)	1.496(11)	C(31)-H(31A)	0.9900
C(27)-H(27A)	0.9900	C(31)-H(31B)	0.9900
C(27)-H(27B)	0.9900	C(32)-C(33)	1.508(11)
C(28)-C(29)	1.480(13)	C(32)-H(32A)	0.9900
C(28)-H(28A)	0.9900	C(32)-H(32B)	0.9900
C(28)-H(28B)	0.9900	C(33)-C(34)	1.499(11)
C(29)-C(30)	1.447(12)	C(33)-H(33A)	0.9900
C(29)-H(29A)	0.9900	C(33)-H(33B)	0.9900
C(29)-H(29B)	0.9900	C(34)-H(34A)	0.9900
C(30)-H(30A)	0.9900	C(34)-H(34B)	0.9900
C(30)-H(30B)	0.9900		
C(31)-C(32)	1.403(11)		

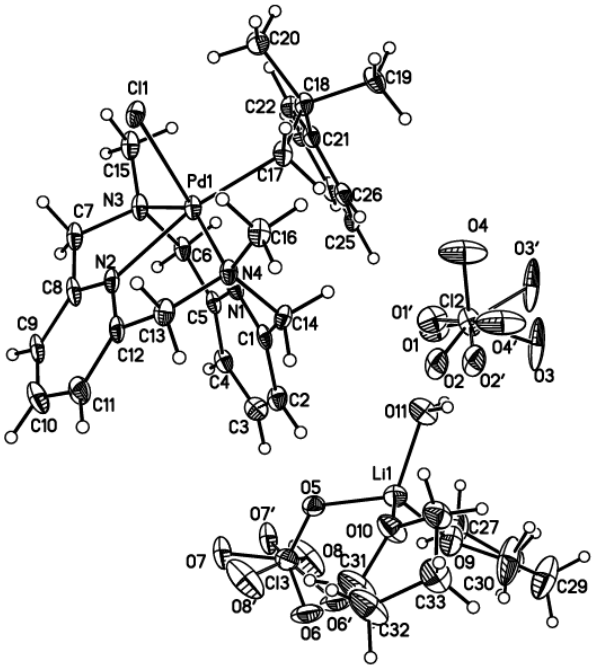

Figure S43. Projection view of [**1**$^{+}$] with 30% thermal ellipsoids (disorder component omitted for clarity)

Table S11. Crystal data and structure refinement for **[2]**.

Identification code	1
Empirical formula	$C_{26}H_{32}N_4Pd$
Formula weight	506.95
Temperature/K	100.0
Crystal system	orthorhombic
Space group	$P2_12_12_1$
a/Å	8.9688(3)
b/Å	15.8749(6)
c/Å	16.3925(5)
α/°	90
β/°	90
γ/°	90
Volume/Å^3	2333.94(14)
Z	4
ρ_{calc}g/cm^3	1.443
μ/mm^{-1}	0.815
F(000)	1048.0
Crystal size/mm^3	0.215 × 0.084 × 0.065
Radiation	MoKα (λ = 0.71073)
2Θ range for data collection/°	4.542 to 50.048
Index ranges	$-10 \leq h \leq 10$, $-18 \leq k \leq 18$, $-19 \leq l \leq 19$
Reflections collected	26114
Independent reflections	4119 [R_{int} = 0.0359, R_{sigma} = 0.0238]
Data/restraints/parameters	4119/3/285
Goodness-of-fit on F^2	1.379
Final R indexes [I>=2σ (I)]	R_1 = 0.0396, wR_2 = 0.0931
Final R indexes [all data]	R_1 = 0.0403, wR_2 = 0.0940
Largest diff. peak/hole / e Å^{-3}	0.60/-1.23
Flack parameter	0.007(12)

Table S12. Fractional Atomic Coordinates (×10^4) and Equivalent Isotropic Displacement Parameters (Å^2×10^3) for **[2]**. U_{eq} is defined as 1/3 of of the trace of the orthogonalised U_{IJ} tensor.

Atom	x	y	z	U(eq)
Pd1	8565.8(7)	4103.8(4)	6070.7(3)	14.63(14)
N1	6468(9)	3926(4)	5440(3)	17.5(14)
N2	8731(8)	5060(4)	5139(4)	17.4(14)
N3	5855(8)	5850(5)	6198(4)	27.9(16)
N4	8873(9)	3310(5)	3987(5)	37(2)

C1	7818(13)	2931(6)	4562(6)	36(3)
C2	6449(13)	3439(5)	4759(4)	23.6(18)
C3	5197(12)	3400(6)	4261(5)	33(3)
C4	3984(11)	3878(7)	4449(5)	39(3)
C5	3982(10)	4383(7)	5137(5)	35(3)
C6	5257(10)	4401(6)	5619(5)	23(2)
C7	5381(10)	4983(6)	6348(5)	27(2)
C8	4911(12)	6322(7)	5633(6)	36(3)
C9	7449(9)	6008(5)	6093(6)	25.3(18)
C10	8141(9)	5822(6)	5262(5)	20.0(17)
C11	8076(11)	6413(6)	4638(6)	30(2)
C12	8613(11)	6226(6)	3877(6)	34(2)
C13	9215(11)	5432(7)	3756(5)	33(2)
C14	9261(10)	4852(7)	4392(5)	28(2)
C15	9869(11)	3966(7)	4273(5)	37(3)
C16	8225(13)	3474(7)	3171(5)	42(3)
C17	8465(11)	3229(4)	6943(4)	15.5(15)
C18	7419(9)	2554(5)	6983(5)	16.1(17)
C19	7516(10)	1950(5)	7589(5)	22.6(19)
C20	8655(12)	1983(5)	8171(5)	24.4(18)
C21	9655(10)	2653(5)	8155(5)	21.4(19)
C22	9563(9)	3261(5)	7555(5)	14.0(17)
C23	10559(9)	4026(6)	7506(4)	15.9(16)
C24	10603(9)	4280(5)	6599(5)	17.9(19)
C25	9810(11)	4756(6)	7982(5)	24(2)
C26	12143(10)	3911(7)	7853(6)	32(3)

Table S13. Bond Lengths for **[2]**.

Atom	Atom	Length/Å	Atom	Atom	Length/Å
Pd1	N1	2.165(8)	C5	C6	1.391(12)
Pd1	N2	2.158(6)	C6	C7	1.515(12)
Pd1	C17	1.996(7)	C9	C10	1.525(12)
Pd1	C24	2.042(8)	C10	C11	1.390(12)
N1	C2	1.358(9)	C11	C12	1.370(14)
N1	C6	1.354(12)	C12	C13	1.385(14)
N2	C10	1.336(11)	C13	C14	1.392(13)
N2	C14	1.354(11)	C14	C15	1.521(15)
N3	C7	1.461(13)	C17	C18	1.426(12)
N3	C8	1.461(11)	C17	C22	1.406(11)

N3	C9	1.462(11)	C18	C19	1.383(11)
N4	C1	1.465(14)	C19	C20	1.399(13)
N4	C15	1.449(14)	C20	C21	1.391(13)
N4	C16	1.482(11)	C21	C22	1.381(11)
C1	C2	1.503(15)	C22	C23	1.510(11)
C2	C3	1.390(14)	C23	C24	1.541(10)
C3	C4	1.362(15)	C23	C25	1.551(12)
C4	C5	1.383(14)	C23	C26	1.541(11)

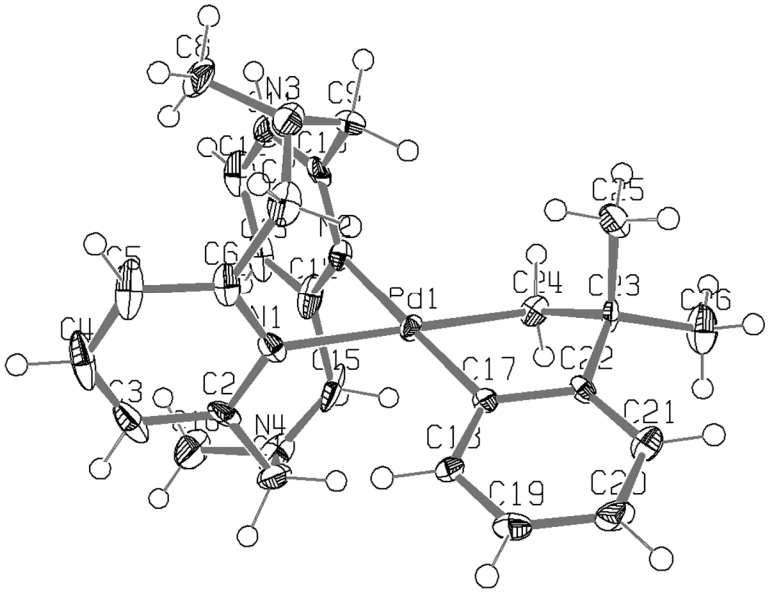

Figure S44. Projection view of **[2]** with 50% thermal ellipsoids

Table S14. Crystal data and structure refinement for **[2$^+$]**.

Identification code	l5213/lt/x8/100K/FT-041713-cyclo	
Empirical formula	C_{28} H_{35} Cl N_5 O_4 Pd	
Formula weight	647.46	
Temperature	100(2) K	
Wavelength	0.71073 Å	
Crystal system	Orthorhombic	
Space group	P 2_1 2_1 2_1	
Unit cell dimensions	a = 11.3400(10) Å	α= 90°.
	b = 12.2808(10) Å	β= 90°.
	c = 20.326(2) Å	γ = 90°.
Volume	2830.7(4) Å^3	

Z	4
Density (calculated)	1.519 Mg/m^3
Absorption coefficient	0.793 mm^{-1}
F(000)	1332
Crystal size	0.331 x 0.218 x 0.069 mm^3
Theta range for data collection	1.937 to 28.412°.
Index ranges	$-15 \leqslant h \leqslant 15$, $-16 \leqslant k \leqslant 16$, $-27 \leqslant l \leqslant 27$
Reflections collected	53968
Independent reflections	7095 [R(int) = 0.0557]
Completeness to theta = 25.242°	100.0 %
Absorption correction	Semi-empirical from equivalents
Max. and min. transmission	0.9583 and 0.8697
Refinement method	Full-matrix least-squares on F^2
Data / restraints / parameters	7095 / 48 / 370
Goodness-of-fit on F^2	1.018
Final R indices [I>2sigma(I)]	R1 = 0.0249, wR2 = 0.0508
R indices (all data)	R1 = 0.0290, wR2 = 0.0524
Absolute structure parameter	-0.022(10)
Extinction coefficient	n/a
Largest diff. peak and hole	0.286 and -0.492 $e.Å^{-3}$

Table S15. Atomic coordinates (x 10^4) and equivalent isotropic displacement parameters ($Å^2$x 10^3) for **[2$^+$]**. U(eq) is defined as one third of the trace of the orthogonalized U^{ij} tensor.

	x	y	z	U(eq)
Pd(1)	9126(1)	9544(1)	1730(1)	10(1)
Cl(1)	6450(1)	3350(1)	1078(1)	18(1)
O(1)	6387(8)	3556(6)	1768(2)	36(2)
O(2)	6519(6)	4336(2)	696(2)	31(1)
O(3)	7500(4)	2743(6)	954(3)	49(1)
O(4)	5431(6)	2736(4)	890(3)	45(1)
O(1')	6320(80)	3810(60)	1713(17)	36(2)
O(2')	6040(50)	4367(19)	840(20)	31(1)

O(3')	7650(20)	3140(50)	970(30)	49(1)
O(4')	5820(50)	2540(30)	730(20)	45(1)
N(1)	10563(2)	8595(2)	1337(1)	12(1)
N(2)	10509(2)	10737(2)	1649(1)	12(1)
N(3)	9101(2)	9973(2)	604(1)	15(1)
N(4)	10346(2)	9203(2)	2663(1)	14(1)
C(1)	11380(3)	8244(2)	1763(2)	14(1)
C(2)	12498(3)	7943(3)	1551(2)	20(1)
C(3)	12761(3)	8034(3)	890(2)	24(1)
C(4)	11920(3)	8426(3)	460(2)	22(1)
C(5)	10819(3)	8705(2)	702(2)	15(1)
C(6)	9821(3)	9116(3)	279(2)	17(1)
C(7)	9657(3)	11067(3)	579(2)	16(1)
C(8)	10672(3)	11183(2)	1055(2)	13(1)
C(9)	11704(3)	11726(3)	904(2)	18(1)
C(10)	12575(3)	11801(3)	1379(2)	20(1)
C(11)	12416(3)	11303(3)	1977(2)	17(1)
C(12)	11368(3)	10751(2)	2100(2)	14(1)
C(13)	11120(3)	10168(2)	2730(2)	17(1)
C(14)	11006(3)	8210(2)	2466(2)	16(1)
C(15)	7932(3)	10024(3)	293(2)	22(1)
C(16)	9753(3)	8978(3)	3289(2)	19(1)
C(17)	7807(2)	8472(2)	1713(2)	13(1)
C(18)	7902(3)	7468(3)	1402(2)	15(1)
C(19)	6918(3)	6792(3)	1341(2)	18(1)
C(20)	5844(3)	7125(3)	1588(2)	22(1)
C(21)	5740(3)	8122(3)	1903(2)	22(1)
C(22)	6715(3)	8801(3)	1965(2)	15(1)
C(23)	6680(3)	9903(2)	2296(2)	15(1)
C(24)	7823(2)	10510(3)	2109(2)	17(1)
C(25)	5612(3)	10572(3)	2070(2)	25(1)
C(26)	6608(3)	9736(3)	3041(2)	20(1)
N(1S)	10104(3)	6158(3)	446(2)	44(1)
C(1S)	9773(3)	5413(3)	179(2)	26(1)
C(2S)	9321(3)	4459(3)	-151(2)	38(1)

Table S16. Bond lengths [Å] for **[2$^+$]**.

Pd(1)-C(17)	1.994(3)	C(4)-H(4)	0.9500
Pd(1)-C(24)	2.045(3)	C(5)-C(6)	1.508(5)
Pd(1)-N(2)	2.152(2)	C(6)-H(6A)	0.9900
Pd(1)-N(1)	2.156(2)	C(6)-H(6B)	0.9900
Pd(1)-N(3)	2.350(2)	C(7)-C(8)	1.510(4)
Pd(1)-N(4)	2.383(3)	C(7)-H(7A)	0.9900
Cl(1)-O(3')	1.41(2)	C(7)-H(7B)	0.9900
Cl(1)-O(2')	1.416(18)	C(8)-C(9)	1.382(4)
Cl(1)-O(1')	1.42(2)	C(9)-C(10)	1.385(5)
Cl(1)-O(4')	1.419(19)	C(9)-H(9)	0.9500
Cl(1)-O(1)	1.426(4)	C(10)-C(11)	1.371(5)
Cl(1)-O(3)	1.427(3)	C(10)-H(10)	0.9500
Cl(1)-O(4)	1.431(3)	C(11)-C(12)	1.392(4)
Cl(1)-O(2)	1.440(3)	C(11)-H(11)	0.9500
N(1)-C(5)	1.331(4)	C(12)-C(13)	1.494(4)
N(1)-C(1)	1.339(4)	C(13)-H(13A)	0.9900
N(2)-C(12)	1.338(4)	C(13)-H(13B)	0.9900
N(2)-C(8)	1.338(4)	C(14)-H(14A)	0.9900
N(3)-C(15)	1.470(4)	C(14)-H(14B)	0.9900
N(3)-C(6)	1.486(4)	C(15)-H(15A)	0.9800
N(3)-C(7)	1.486(4)	C(15)-H(15B)	0.9800
N(4)-C(16)	1.466(4)	C(15)-H(15C)	0.9800
N(4)-C(13)	1.482(4)	C(16)-H(16A)	0.9800
N(4)-C(14)	1.485(4)	C(16)-H(16B)	0.9800
C(1)-C(2)	1.389(4)	C(16)-H(16C)	0.9800
C(1)-C(14)	1.491(5)	C(17)-C(18)	1.389(4)
C(2)-C(3)	1.380(5)	C(17)-C(22)	1.399(4)
C(2)-H(2)	0.9500	C(18)-C(19)	1.396(4)
C(3)-C(4)	1.381(5)	C(18)-H(18)	0.9500
C(3)-H(3)	0.9500	C(19)-C(20)	1.379(5)
C(4)-C(5)	1.385(5)	C(19)-H(19)	0.9500

C(20)-C(21)	1.387(5)	C(25)-H(25B)	0.9800
C(20)-H(20)	0.9500	C(25)-H(25C)	0.9800
C(21)-C(22)	1.391(4)	C(26)-H(26A)	0.9800
C(21)-H(21)	0.9500	C(26)-H(26B)	0.9800
C(22)-C(23)	1.512(4)	C(26)-H(26C)	0.9800
C(23)-C(26)	1.531(4)	N(1S)-C(1S)	1.129(5)
C(23)-C(25)	1.534(4)	C(1S)-C(2S)	1.445(5)
C(23)-C(24)	1.544(4)	C(2S)-H(2SA)	0.9800
C(24)-H(24A)	0.9900	C(2S)-H(2SB)	0.9800
C(24)-H(24B)	0.9900	C(2S)-H(2SC)	0.9800
C(25)-H(25A)	0.9800		

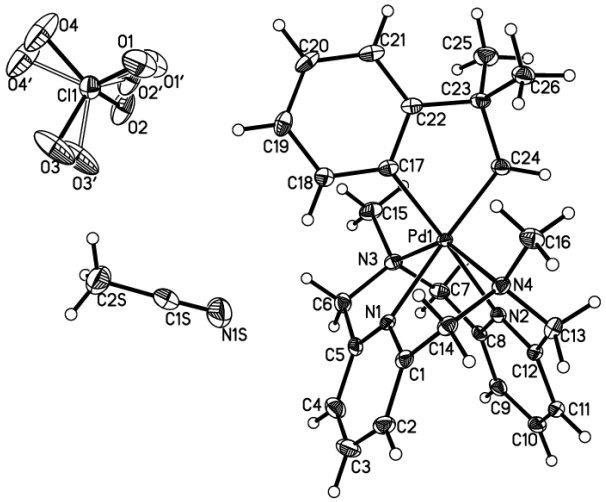

Figure S45. Projection view of [$\mathbf{2}^{+}$] with 50% thermal ellipsoids.

Table S17. Crystal data and structure refinement for [$\mathbf{2}^{2+}$].

Identification code	l6813/lt/x8/173K/FT-0515-1
Empirical formula	C_{30} H_{38} Cl_2 N_6 O_8 Pd
Formula weight	787.96
Temperature	173(2) K
Wavelength	0.71073 Å

Crystal system	Orthorhombic	
Space group	P m n 2_1	
Unit cell dimensions	a = 17.1932(5) Å	α= 90°.
	b = 11.4548(3) Å	β= 90°.
	c = 8.6473(3) Å	γ = 90°.
Volume	1703.04(9) $Å^3$	
Z	2	
Density (calculated)	1.537 Mg/m^3	
Absorption coefficient	0.759 mm^{-1}	
F(000)	808	
Crystal size	0.354 x 0.316 x 0.092 mm^3	
Theta range for data collection	2.136 to 31.074°.	
Index ranges	-24⩽h⩽24, -16⩽k⩽16, -12⩽l⩽11	
Reflections collected	37189	
Independent reflections	5494 [R(int) = 0.0439]	
Completeness to theta = 25.242°	99.9 %	
Absorption correction	Semi-empirical from equivalents	
Max. and min. transmission	0.7462 and 0.6809	
Refinement method	Full-matrix least-squares on F^2	
Data / restraints / parameters	5494 / 7 / 234	
Goodness-of-fit on F^2	1.049	
Final R indices [I>2sigma(I)]	R1 = 0.0267, wR2 = 0.0610	
R indices (all data)	R1 = 0.0314, wR2 = 0.0634	
Absolute structure parameter	0.028(10)	
Extinction coefficient	n/a	
Largest diff. peak and hole	0.700 and -0.453 e.$Å^{-3}$	

Table S18. Atomic coordinates (x 10^4) and equivalent isotropic displacement parameters ($Å^2$x 10^3) for **[2^{2+}]**. U(eq) is defined as one third of the trace of the orthogonalized U^{ij} tensor.

	x	y	z	U(eq)
Pd(1)	10000	6481(1)	233(1)	17(1)
Cl(1)	7810(1)	7094(1)	5416(1)	33(1)

O(1)	7122(2)	7099(3)	6323(5)	75(1)
O(2)	8101(2)	5917(2)	5387(4)	56(1)
O(3)	7629(2)	7417(2)	3875(3)	53(1)
O(4)	8350(2)	7877(3)	6074(4)	70(1)
N(1)	10000	5207(4)	1923(5)	22(1)
N(2)	10000	5052(4)	-1218(5)	20(1)
N(3)	8789(1)	6091(2)	280(4)	22(1)
C(1)	9316(2)	4749(3)	2330(4)	23(1)
C(2)	8640(2)	5470(3)	1795(4)	25(1)
C(3)	8638(2)	5291(3)	-1076(5)	28(1)
C(4)	9316(2)	4525(3)	-1437(4)	23(1)
C(5)	9297(2)	3760(3)	3246(4)	30(1)
C(6)	10000	3284(4)	3697(6)	33(1)
C(7)	9295(2)	3395(3)	-2024(4)	31(1)
C(8)	10000	2855(4)	-2326(5)	34(1)
C(9)	10000	7859(5)	1669(6)	21(1)
C(10)	10000	7734(4)	3267(5)	27(1)
C(11)	10000	8719(4)	4184(5)	31(1)
C(12)	8215(1)	7065(2)	194(5)	30(1)
C(13)	10000	9925(4)	1924(6)	30(1)
C(14)	10000	8946(4)	957(6)	21(1)
C(15)	10000	9016(4)	-788(6)	23(1)
C(16)	10000	7746(4)	-1454(6)	21(1)
C(17)	9274(2)	9678(2)	-1340(4)	33(1)
C(18)	10000	9814(4)	3511(6)	32(1)
N(1S)	6558(2)	8565(2)	10268(8)	54(1)
C(1S)	6776(2)	9126(3)	9275(5)	42(1)
C(2S)	7047(2)	9830(3)	7980(6)	51(1)

Table S19. Bond lengths [Å] for **[2^{2+}]**.

Pd(1)-C(9)	2.008(5)	Pd(1)-N(3)	2.1305(18)
Pd(1)-C(16)	2.056(5)	Pd(1)-N(3)#1	2.1305(18)
Pd(1)-N(2)	2.063(4)	Cl(1)-O(4)	1.410(3)
Pd(1)-N(1)	2.066(4)	Cl(1)-O(3)	1.417(3)

Cl(1)-O(1)	1.421(3)	C(9)-C(10)	1.390(6)
Cl(1)-O(2)	1.438(2)	C(10)-C(11)	1.379(6)
N(1)-C(1)	1.335(4)	C(10)-H(10)	0.9500
N(1)-C(1)#1	1.335(4)	C(11)-C(18)	1.383(6)
N(2)-C(4)#1	1.335(4)	C(11)-H(11)	0.9500
N(2)-C(4)	1.335(4)	C(12)-H(12A)	0.9800
N(3)-C(12)	1.490(3)	C(12)-H(12B)	0.9800
N(3)-C(3)	1.511(5)	C(12)-H(12C)	0.9800
N(3)-C(2)	1.513(5)	C(13)-C(18)	1.378(7)
C(1)-C(5)	1.382(4)	C(13)-C(14)	1.399(6)
C(1)-C(2)	1.500(5)	C(13)-H(13)	0.9500
C(2)-H(2A)	0.9900	C(14)-C(15)	1.511(6)
C(2)-H(2B)	0.9900	C(15)-C(17)#1	1.536(4)
C(3)-C(4)	1.492(5)	C(15)-C(17)	1.536(4)
C(3)-H(3A)	0.9900	C(15)-C(16)	1.565(7)
C(3)-H(3B)	0.9900	C(16)-H(16A)	0.9900
C(4)-C(7)	1.390(4)	C(16)-H(16B)	0.9900
C(5)-C(6)	1.383(4)	C(17)-H(17A)	0.9800
C(5)-H(5)	0.9500	C(17)-H(17B)	0.9800
C(6)-C(5)#1	1.383(4)	C(17)-H(17C)	0.9800
C(6)-H(6)	0.9500	C(18)-H(18)	0.9500
C(7)-C(8)	1.385(4)	N(1S)-C(1S)	1.137(6)
C(7)-H(7)	0.9500	C(1S)-C(2S)	1.457(6)
C(8)-C(7)#1	1.385(4)	C(2S)-H(2SA)	0.9800
C(8)-H(8)	0.9500	C(2S)-H(2SB)	0.9800
C(9)-C(14)	1.389(7)	C(2S)-H(2SC)	0.9800

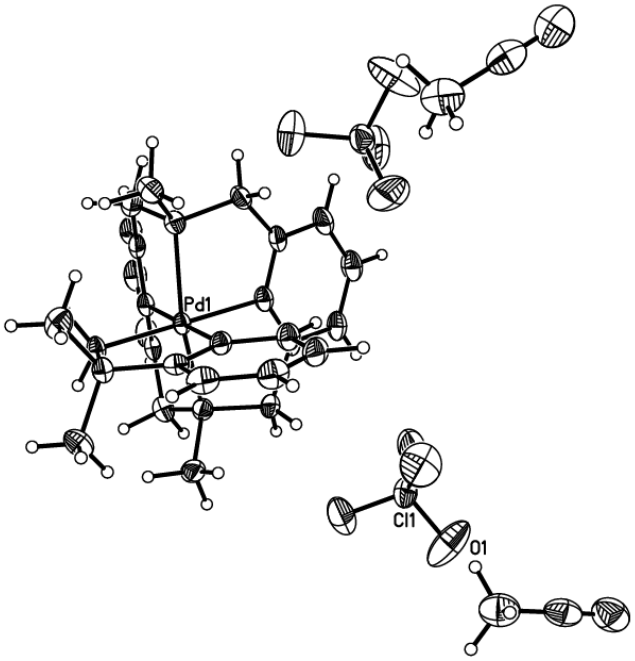

Figure S46. Projection view of [$\mathbf{2}^{2+}$](ClO_4)$_2$ with 50% thermal ellipsoids.

VIII. Computational Details

Geometry optimizations and frequency calculations were performed at the M06 level of theory utilizing the Stuttgart/Dresden ECP (SDD) basis set using the Gaussian 16 package.[8-10] Acetonitrile was used as the solvent, and solvation was modeled utilizing the SMD variant of the IEFPCM SCRF model.[11] The C-H activation transition state structures contained imaginary frequencies and exhibited optimized structures consistent with expected cyclic transition states for concerted metalation-deprotonation processes. The kinetic isotope effect for the C-H activation transition state was determined by calculating the $\Delta G_D^{\ddagger} - \Delta G_H^{\ddagger}$ value from the calculated force constants for the protonated and deuterated analogues of the intermediate and the transition state geometries and using that to get the KIE:

$$\text{KIE} = \frac{k_H}{k_D} = e^{-(\Delta G_D^{\ddagger} - \Delta G_H^{\ddagger})/RT}$$

The general reaction profile proceeds as follows: 1) dissociation of axial amines (I → II); 2) rearrangement of the bound acetate from the equatorial to the axial position (II to III via II-TS); 3) the transition state for C-H activation (III → III-TS); 5) loss of acetic acid and formation of the palladacycle **2**$^+$ (III-TS → IV). In addition, a reaction coordinate involving a κ^2- coordination of the ^{Me}N4 ligand is calculated and shown to be significantly higher in energy.

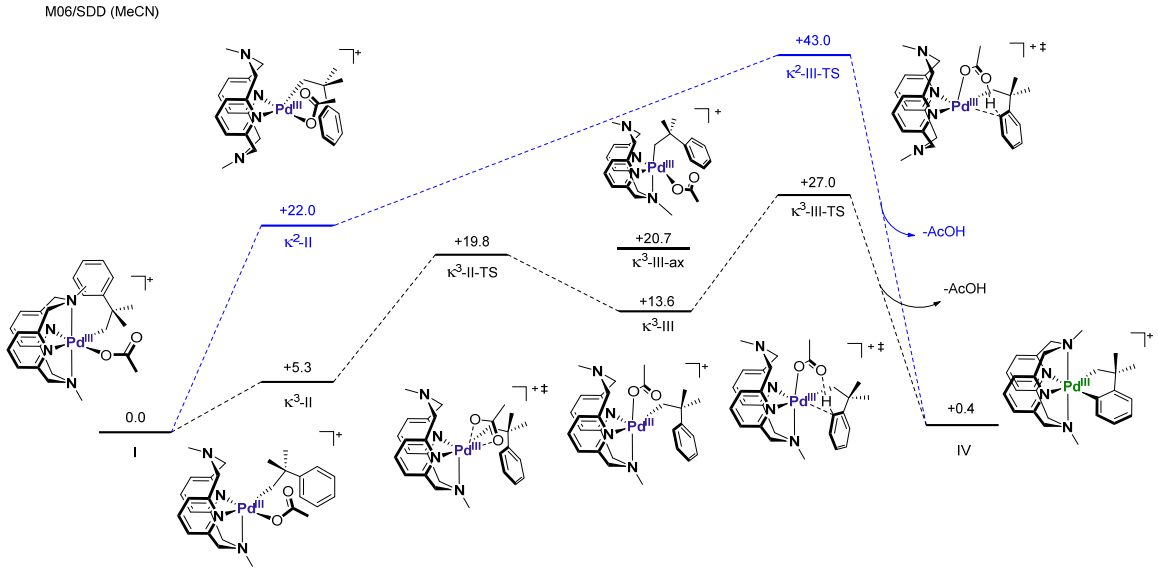

Figure S47. Calculated energy profiles for the conversion of **Int-B** (I) to **2**$^+$ (IV) via two pathways involving either a κ^2- (blue line) or κ^3- (black line) ^{Me}N4 ligand configuration. The free energy values are shown in kcal/mol. The energy of an alternate intermediate, κ^3-III-ax, with the neophyl ligand bound in an axial position is also shown to highlight the higher energy of such a rearranged ligand conformation.

Cartesian coordinates (Å) and energies of optimized complexes obtained by DFT at the M06/SDD level of theory:

I

Energy: -1584.175510 Hartrees

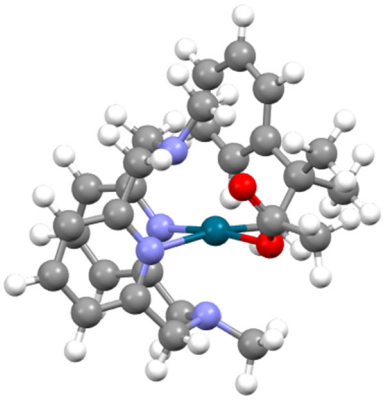

71

MeN4Pd^{III}NeophylOAc

Pd	13.053300	11.769600	2.504900
N	11.416700	12.952300	3.009000
N	11.535600	10.247200	2.834800
N	12.929400	11.543100	4.965600
N	11.880700	11.792000	0.465100
C	10.538300	13.235500	2.013700
C	9.282300	13.771700	2.311000
H	8.592800	13.995600	1.504300
C	8.932400	13.983600	3.651300
H	7.959000	14.390100	3.903500
C	9.832600	13.629100	4.664700
H	9.576700	13.741300	5.712800
C	11.079400	13.101700	4.314300
C	12.104000	12.718600	5.347400
H	12.793700	13.568200	5.465200
H	11.608400	12.551900	6.317700
C	12.225800	10.239000	5.155500
H	11.771600	10.195500	6.158400
H	13.005600	9.470000	5.085200
C	11.197900	9.931400	4.103800
C	9.967200	9.324800	4.383400
H	9.707800	9.077100	5.407100
C	9.085200	9.067500	3.324500
H	8.122100	8.607000	3.517300
C	9.439600	9.435900	2.017500

H	8.764700	9.276600	1.183400
C	10.681800	10.041500	1.804800
C	11.158200	10.483600	0.445700
H	11.867100	9.736500	0.066300
H	10.313300	10.529200	-0.258100
C	10.974100	12.967500	0.594700
H	10.088500	12.847000	-0.046900
H	11.522200	13.846100	0.231000
C	14.166100	11.508500	5.783000
H	14.809500	10.707400	5.407800
H	13.923700	11.322500	6.843700
H	14.687600	12.466800	5.709800
C	12.737000	11.908500	-0.737800
H	13.266800	12.865200	-0.723800
H	12.132500	11.850400	-1.656500
H	13.470200	11.097000	-0.732200
C	14.227400	13.361700	1.869300
H	14.763200	12.864700	1.047200
H	13.493300	14.070100	1.458600
C	15.244000	14.049800	2.783000
C	15.970100	15.104400	1.897600
H	16.477400	14.609500	1.058300
H	16.724100	15.639200	2.492400
H	15.264200	15.841000	1.491800
C	16.298400	13.026100	3.230600
H	15.870500	12.246600	3.871100
H	17.132700	13.502000	3.761800
H	16.713500	12.532800	2.341400
C	14.602200	14.823300	3.938800
C	15.224300	14.926100	5.199100
H	16.146700	14.387200	5.398500
C	14.675200	15.715900	6.222300
H	15.176700	15.771400	7.184600
C	13.487400	16.430900	6.006700
H	13.061000	17.042200	6.796800
C	12.863700	16.353500	4.750600
H	11.947000	16.906300	4.561100
C	13.418100	15.564300	3.733400
H	12.918000	15.534800	2.768000
O	14.570900	10.562900	1.743200
C	15.119800	9.570900	2.415200
O	14.817700	9.242000	3.597000
C	16.210000	8.845700	1.654000
H	17.125700	9.449300	1.682500
H	16.415200	7.875100	2.112200
H	15.929300	8.715000	0.604900

κ^2-II

Energy: -1584.140509

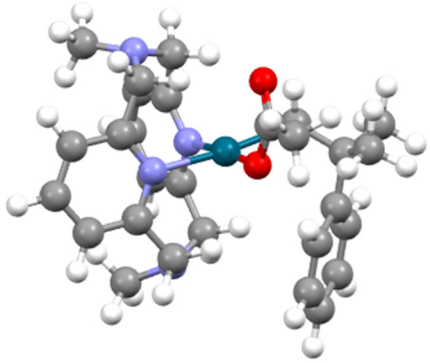

71

κ^2-MeN4Pd^{III}NeophylOAc-equatorial

Pd	10.269900	11.895500	2.724100
N	11.865000	10.741000	1.876300
N	11.820100	13.063200	3.402200
N	12.201800	13.548600	0.139900
N	12.465100	10.271900	5.098800
C	12.444600	9.768300	2.630900
C	13.560800	9.072300	2.147600
H	13.996700	8.288900	2.759500
C	14.086600	9.395300	0.891500
H	14.949900	8.865600	0.503400
C	13.480000	10.409100	0.141300
H	13.852300	10.686700	-0.839800
C	12.362300	11.080400	0.655800
C	11.701800	12.199000	-0.132100
H	11.872600	11.991200	-1.197100
H	10.616900	12.188000	0.047000
C	11.650100	14.327400	1.252000
H	10.567300	14.152400	1.302000
H	11.804000	15.390400	1.023700
C	12.297300	14.061800	2.601900
C	13.410200	14.810200	3.005300
H	13.759600	15.611700	2.362300
C	14.043600	14.521500	4.218300
H	14.903300	15.098200	4.541500
C	13.549300	13.478300	5.007700
H	14.007600	13.222600	5.957600
C	12.433900	12.747500	4.580400
C	11.910800	11.590600	5.412500

H	12.152900	11.811300	6.461200
H	10.817100	11.532600	5.323100
C	11.890400	9.473100	4.013800
H	10.799800	9.617400	4.013500
H	12.094900	8.416300	4.232700
C	13.892600	10.097400	5.343000
H	14.145900	10.515200	6.325300
H	14.542300	10.582200	4.591300
H	14.132100	9.026600	5.351000
C	8.421700	10.631000	5.363100
C	8.922400	9.814900	6.387400
H	9.090300	8.758100	6.197700
C	9.213300	10.359500	7.647800
H	9.600500	9.728700	8.442500
C	8.996700	11.728200	7.869300
H	9.216800	12.163600	8.840000
C	8.486200	12.541700	6.844700
H	8.316800	13.594300	7.051500
C	8.181900	12.005900	5.578100
C	7.640300	12.870400	4.431100
C	8.775800	13.314700	3.533800
H	9.501600	13.964000	4.037400
H	8.494700	13.617300	2.513800
C	6.511600	12.152300	3.671500
H	5.662000	11.986500	4.346300
H	6.820400	11.182500	3.271300
H	6.169800	12.775400	2.833800
C	7.042000	14.212200	4.945400
H	7.790400	14.857800	5.417900
H	6.247400	13.996800	5.672200
H	6.602000	14.761700	4.104500
H	8.216800	10.188800	4.390900
O	8.325100	12.129600	0.461900
C	8.147800	11.003000	1.006000
O	8.858200	10.597400	2.050000
C	7.106200	10.035100	0.514300
H	7.063500	9.140600	1.139000
H	6.128800	10.529800	0.512300
H	7.335700	9.748900	-0.517700
C	13.603200	13.791600	-0.183700
H	13.820700	13.382300	-1.178100
H	13.790500	14.872500	-0.208000
H	14.317500	13.341600	0.531000

κ^3-II

Energy: -1584.708151 Hartrees

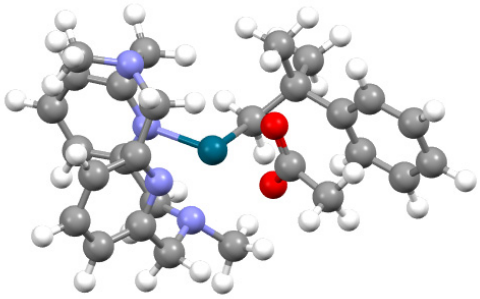

71

κ^3-MeN4Pd^{III}NeophylOAc-equatorial

Pd	10.421400	11.851700	3.593400
N	11.810000	10.796800	2.220100
N	11.967500	13.235600	3.479000
N	11.281000	13.396600	0.201500
N	11.828100	10.908200	5.096300
C	12.765600	10.105800	2.893100
C	13.913700	9.636300	2.250000
C	14.067700	9.882200	0.878300
C	13.083700	10.609500	0.199600
C	11.963200	11.082200	0.902100
C	10.931300	11.970300	0.233900
C	11.031300	14.212400	1.394100
C	12.107400	14.127900	2.463200
C	13.268700	14.909100	2.377800
C	14.298800	14.726600	3.306800
C	14.153300	13.760300	4.310200
C	12.967600	13.026200	4.379200
C	12.727500	12.032300	5.486400
C	12.503100	9.805800	4.343600
C	11.129100	10.325900	6.271900
C	5.968700	11.844100	4.136300
C	5.045900	10.839100	4.473500
C	5.124700	10.189600	5.713200
C	6.138400	10.559900	6.614500
C	7.049300	11.567900	6.275500
C	6.986700	12.226300	5.028400
C	7.953700	13.375300	4.727900
C	9.419700	13.008600	4.995000
C	7.796700	13.943300	3.311200
C	7.620500	14.524400	5.724300

C	12.447900	13.754400	-0.598200
H	14.662600	9.091100	2.814700
H	14.945400	9.521800	0.352400
H	13.173100	10.824400	-0.860700
H	10.816700	11.636900	-0.806400
H	9.966500	11.849200	0.744600
H	10.066500	13.909300	1.820200
H	10.955600	15.260800	1.076900
H	13.350500	15.644200	1.584100
H	15.204900	15.319200	3.245300
H	14.938100	13.574700	5.035300
H	13.686200	11.644500	5.858100
H	12.241000	12.559900	6.316600
H	11.834200	8.937600	4.397800
H	13.439000	9.537200	4.854100
H	10.735900	11.119500	6.911300
H	11.827700	9.714700	6.861300
H	10.303400	9.703200	5.914300
H	5.883700	12.322700	3.165400
H	4.269400	10.564900	3.764100
H	4.412900	9.411800	5.974800
H	6.213400	10.068900	7.581200
H	7.819700	11.842100	6.994600
H	9.544600	12.450900	5.930800
H	10.028700	13.925500	5.024300
H	6.788300	14.351700	3.158300
H	7.985300	13.178400	2.544900
H	8.511300	14.767200	3.174100
H	7.800200	14.224000	6.764400
H	6.563600	14.808400	5.624500
H	8.238900	15.405400	5.506300
H	12.374800	13.267900	-1.578900
H	12.464100	14.840400	-0.753400
H	13.417000	13.462700	-0.150400
O	8.223400	10.854100	1.777900
C	8.311300	10.061300	2.760000
O	9.109000	10.274700	3.790800
C	7.541400	8.765200	2.800000
H	7.380900	8.428800	3.827500
H	6.585100	8.877100	2.281800
H	8.122700	7.995700	2.276700

κ^3-II-TS

Energy: -1584.144048 Hartrees

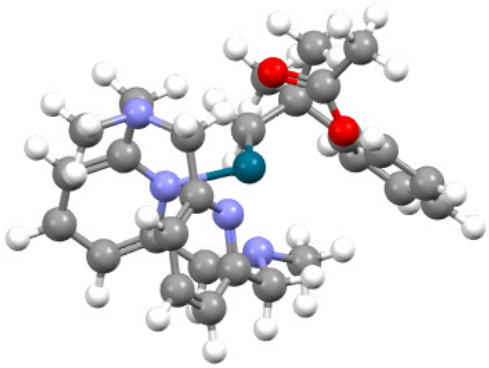

71

κ^3-MeN4Pd^{III}NeophylOAc-isomer-TS

Pd	11.14557900	11.75786700	3.28342800
C	8.22298100	10.66409400	5.32936300
C	7.94209100	9.62569600	6.22836900
C	7.75972300	9.89145400	7.59585300
C	7.85924700	11.21348500	8.05265400
C	8.12300900	12.25641000	7.14878900
C	8.30656200	12.00163300	5.77547200
C	8.58426100	13.12220500	4.76770200
C	10.05772100	13.20155300	4.33122300
C	7.60501700	13.02123100	3.58444500
C	8.35201600	14.52423300	5.39697400
H	8.43145900	10.42275300	4.28027000
H	7.87999300	8.60340500	5.86314000
H	7.54474000	9.08422200	8.29054700
H	7.72376200	11.43781900	9.10736500
H	8.18079000	13.27090800	7.53213400
H	10.70637600	13.36193100	5.20555400
H	10.18214500	14.02142500	3.60478600
H	6.58571300	13.23016700	3.93699900
H	7.60405700	12.02936200	3.12711000
H	7.86448000	13.75528500	2.81030800
H	9.05877000	14.74655100	6.20594200
H	7.33108500	14.58787900	5.79654800
H	8.46356800	15.29648800	4.62563900
N	12.75867000	10.57960800	2.25704400
N	12.77653100	13.11931500	3.31508900
N	12.69570600	13.05162500	-0.02509900

N	12.24359800	10.97361300	5.05760600
C	13.52961400	9.93488700	3.17418500
C	14.80615300	9.46438900	2.86333600
C	15.29837200	9.66128400	1.56475600
C	14.50595900	10.33777700	0.63223500
C	13.23613200	10.81120000	1.00667500
C	12.38854400	11.61500600	0.03948100
C	12.19961500	13.93549700	1.03818900
C	13.07295900	13.94855300	2.28101600
C	14.22914300	14.73998100	2.34189200
C	15.09545900	14.62320800	3.43532200
C	14.79488600	13.71305500	4.45535200
C	13.61290500	12.97262900	4.37263800
C	13.20498200	12.03952300	5.47857800
C	12.91497300	9.73689500	4.52798200
C	11.40375900	10.57551600	6.22092000
C	13.99201000	13.40285600	-0.59831900
H	15.39340200	8.95866900	3.62193600
H	16.28373600	9.30014100	1.29076900
H	14.85304300	10.50573500	-0.38237400
H	12.54330000	11.20598500	-0.96768400
H	11.33199200	11.50067100	0.30415300
H	11.17532800	13.63588700	1.29461200
H	12.16960200	14.95765800	0.63883600
H	14.43943200	15.42648800	1.52835600
H	15.99796800	15.22229000	3.48485100
H	15.45210500	13.57540400	5.30705300
H	14.09384900	11.57864100	5.93096000
H	12.71490300	12.63153600	6.26171700
H	12.13516200	8.96785100	4.45502900
H	13.66584500	9.39583000	5.25367800
H	10.85903700	11.44219300	6.60383900
H	12.04770800	10.16973700	7.01526700
H	10.68998100	9.81069800	5.90555400
H	14.13333100	12.84937000	-1.53486200
H	14.01139400	14.47625400	-0.82515600
H	14.85611600	13.18164700	0.05644900
O	9.46559300	11.86667100	1.20642100
C	8.90724800	10.75245500	1.53395100
O	9.20244100	10.11338900	2.62363000
C	7.81795000	10.19682300	0.64970100
H	7.70399000	9.12024500	0.79689600
H	6.87091600	10.68513000	0.91408900
H	8.02721600	10.41478600	-0.40098500

κ^3-III

Energy: -1584.153779 Hartrees

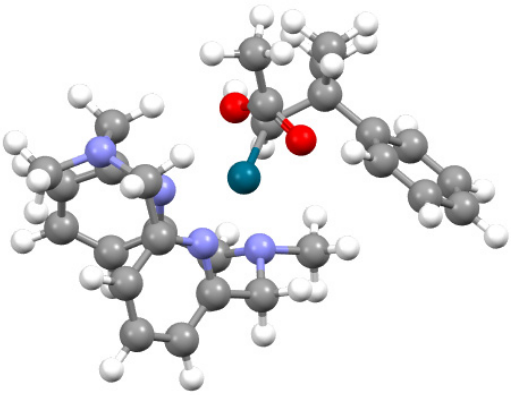

71

κ^3-MeN4Pd^{III}NeophylOAc-axial

Pd	10.053600	11.876800	3.436400
C	7.428800	10.529700	5.054700
C	7.269600	9.328400	5.757800
C	7.003500	9.344000	7.137300
C	6.897700	10.576700	7.797000
C	7.054300	11.779100	7.086000
C	7.327100	11.779500	5.705600
C	7.494600	13.071700	4.895800
C	8.942400	13.319200	4.424200
C	6.483300	13.069800	3.731800
C	7.183300	14.330800	5.744000
H	7.643400	10.482700	3.985500
H	7.353100	8.381900	5.230000
H	6.877200	8.413900	7.683900
H	6.687200	10.607500	8.862600
H	6.963100	12.715400	7.628200
H	9.599800	13.561500	5.271600
H	8.965700	14.126300	3.677300
H	5.463500	13.117500	4.138100
H	6.551000	12.169700	3.113700
H	6.642800	13.943800	3.086500
H	7.868700	14.439700	6.594000
H	6.154100	14.290500	6.124800
H	7.275600	15.227000	5.117000
N	11.669500	10.573600	2.455600
N	11.836000	13.224600	3.170000
N	11.739700	12.770700	-0.148300

N	11.190000	11.328700	5.186700
C	12.420200	10.024800	3.450900
C	13.706600	9.531900	3.228000
C	14.240500	9.608100	1.933200
C	13.473700	10.186400	0.918000
C	12.188200	10.681700	1.205200
C	11.377400	11.373000	0.123900
C	11.324400	13.810900	0.804900
C	12.201100	13.886800	2.041600
C	13.433000	14.560400	1.992400
C	14.316600	14.475800	3.073500
C	13.952100	13.718800	4.192200
C	12.691900	13.114500	4.217700
C	12.236600	12.374000	5.441000
C	11.781400	9.993100	4.805500
C	10.442000	11.123800	6.466100
C	13.015700	12.982500	-0.826400
H	14.271000	9.106500	4.050700
H	15.235600	9.229900	1.725500
H	13.850700	10.257600	-0.097400
H	11.513800	10.814700	-0.811500
H	10.321500	11.333700	0.395800
H	10.284700	13.625300	1.091100
H	11.383700	14.775800	0.285400
H	13.686300	15.131600	1.105200
H	15.277400	14.977700	3.038900
H	14.618000	13.601700	5.040500
H	13.095100	11.912600	5.948400
H	11.802900	13.100600	6.139500
H	10.948600	9.277000	4.802700
H	12.502800	9.688100	5.575000
H	9.946600	12.050300	6.764700
H	11.152800	10.826100	7.250000
H	9.694800	10.338000	6.334900
H	13.085800	12.300100	-1.682700
H	13.058600	14.012600	-1.201800
H	13.909200	12.818500	-0.196000
O	8.829200	12.330400	1.807800
C	8.075400	11.357600	1.321300
O	8.035500	10.195000	1.813500
C	7.271500	11.752200	0.107800
H	6.663400	10.914900	-0.240600
H	6.625100	12.603100	0.350600
H	7.949400	12.073500	-0.692500

κ^3-III-ax

Energy: -1584.142494 Hartrees

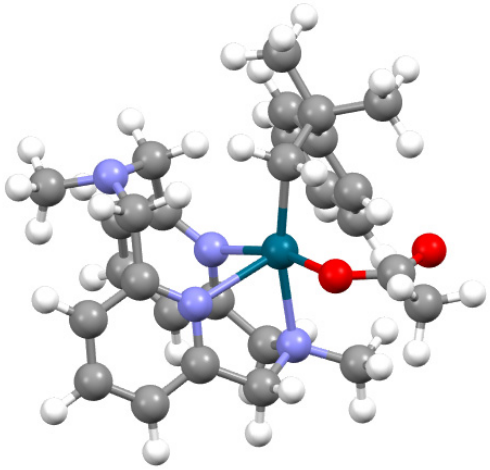

71

κ^3-MeN4Pd^{III}OAcNeophyl-axial

Pd	10.032700	11.468800	3.398300
C	8.480500	13.255300	4.670400
C	9.084600	13.935800	5.739900
C	9.506900	15.263200	5.580100
C	9.316500	15.902900	4.343000
C	8.705300	15.226300	3.274100
C	8.278400	13.897100	3.422800
H	9.214000	13.434300	6.696200
H	9.970700	15.795200	6.405400
H	9.639500	16.931900	4.211100
H	8.566700	15.745900	2.329900
C	7.622400	13.081500	2.304800
C	8.531000	11.880000	1.940200
C	6.254000	12.562200	2.796600
C	7.363900	13.913600	1.037100
H	9.007500	12.002200	0.966200
H	7.991400	10.926100	1.962300
H	5.614000	13.401800	3.101000
H	6.358600	11.875100	3.644700
H	5.751300	12.022800	1.982200
H	8.280700	14.337600	0.609000
H	6.672200	14.739800	1.252000
H	6.900800	13.275400	0.273700
H	8.105400	12.233600	4.793500
N	11.919100	10.484200	2.386700

N	11.544000	13.036300	3.338100
N	11.748300	12.869400	-0.007300
N	11.255300	10.862700	5.173200
C	12.715000	9.963900	3.361000
C	14.053600	9.642900	3.118800
C	14.584900	9.856400	1.840400
C	13.764400	10.408200	0.853400
C	12.431300	10.738700	1.157200
C	11.567300	11.415800	0.112300
C	11.137200	13.765000	0.983500
C	11.877200	13.858300	2.299800
C	12.955600	14.749600	2.403000
C	13.751700	14.757900	3.551100
C	13.458200	13.847700	4.568800
C	12.352300	13.001000	4.440000
C	12.038600	12.063200	5.571100
C	12.096800	9.721900	4.706900
C	10.454100	10.406100	6.342500
C	13.037500	13.304500	-0.540700
H	14.656700	9.233900	3.922300
H	15.617700	9.605700	1.623900
H	14.134700	10.586300	-0.151200
H	11.815800	10.980800	-0.864400
H	10.519000	11.190200	0.319000
H	10.113300	13.450100	1.168300
H	11.105100	14.769400	0.541000
H	13.159800	15.416400	1.571600
H	14.591200	15.438400	3.640400
H	14.068700	13.783300	5.463000
H	12.972000	11.763500	6.071300
H	11.443600	12.612800	6.312400
H	11.432600	8.851200	4.638200
H	12.878000	9.500300	5.448600
H	9.742500	11.183500	6.630700
H	11.120800	10.189700	7.191600
H	9.907200	9.495700	6.086900
H	13.278400	12.712400	-1.432100
H	12.969800	14.359800	-0.833100
H	13.880900	13.205900	0.168000
O	9.047400	9.659200	3.571200
C	8.008200	9.400800	4.351200
O	7.386700	10.260400	5.033300
C	7.643400	7.934300	4.390100
H	8.429900	7.384600	4.921900
H	6.692600	7.791700	4.908200
H	7.583400	7.527900	3.376300

κ^2-TS

Energy: -1584.10696 Hartrees

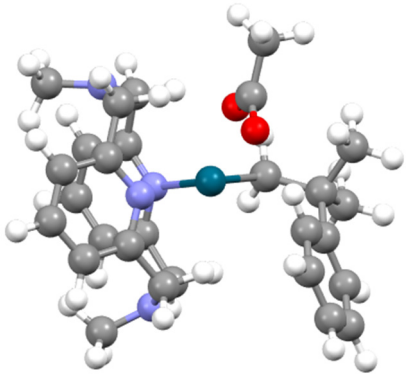

71

κ^2-MeN4Pd^{III}NeophylOAc-TS

Pd	10.238900	12.094800	2.803200
N	11.903900	10.803700	1.858100
N	11.948100	13.289500	3.321300
N	12.375600	13.525800	-0.007000
N	12.559700	10.516600	5.160900
C	12.474400	9.870000	2.687000
C	13.577400	9.103800	2.275600
H	13.993400	8.363400	2.949900
C	14.122000	9.314300	0.996400
H	14.959900	8.719600	0.653000
C	13.563300	10.310600	0.170100
H	13.974700	10.513300	-0.808800
C	12.451100	11.049100	0.621800
C	11.861400	12.160700	-0.246300
H	12.063100	11.913000	-1.297100
H	10.790200	12.186200	-0.114000
C	11.792700	14.368200	1.059100
H	10.722600	14.166800	1.114100
H	11.926800	15.415700	0.762500
C	12.433200	14.213700	2.445400
C	13.573900	14.966400	2.783000
H	13.931800	15.724700	2.080400
C	14.242000	14.717300	3.989900
H	15.176500	15.229500	4.225900
C	13.745400	13.736100	4.861600
H	14.237000	13.514100	5.802200
C	12.583800	13.022400	4.510800
C	12.065900	11.888500	5.454900

H	12.404200	12.134800	6.408700
H	10.983300	11.854300	5.446400
C	11.920500	9.695600	4.099700
H	10.849200	9.917000	4.110500
H	12.034300	8.640500	4.376400
C	13.996800	10.265000	5.378300
H	14.293700	10.704300	6.342100
H	14.650200	10.691900	4.598500
H	14.177800	9.186300	5.419900
C	7.956800	10.433800	3.962800
C	8.017900	9.072400	4.319300
H	8.181800	8.326500	3.547500
C	7.822100	8.671700	5.660800
H	7.818600	7.618600	5.932400
C	7.605300	9.660200	6.642400
H	7.436200	9.369700	7.677300
C	7.591900	11.028000	6.295100
H	7.426500	11.759200	7.081700
C	7.763000	11.441000	4.950000
C	7.697900	12.917300	4.504100
C	9.047900	13.409900	3.922700
H	9.752400	13.645500	4.720900
H	8.923400	14.262000	3.242200
C	6.533600	13.092300	3.485200
H	6.448900	14.140000	3.170500
H	5.584100	12.796000	3.945500
H	6.670800	12.475600	2.583100
C	7.432600	13.884400	5.699400
H	8.210200	13.820700	6.444000
H	6.479700	13.673300	6.168300
H	7.416000	14.923400	5.331700
H	8.018100	10.682400	2.907800
C	13.789200	13.748300	-0.334600
H	14.002500	13.305600	-1.315600
H	13.987000	14.825500	-0.391900
H	14.496100	13.313500	0.396100
O	9.058900	12.783500	1.185400
C	8.423200	11.894200	0.402900
O	8.394400	10.638700	0.645000
C	7.714400	12.512500	-0.803100
H	8.287600	13.347200	-1.226500
H	7.550200	11.745300	-1.573600
H	6.730700	12.897500	-0.479000

κ^3-III-TS

Energy: -1584.132486 Hartrees

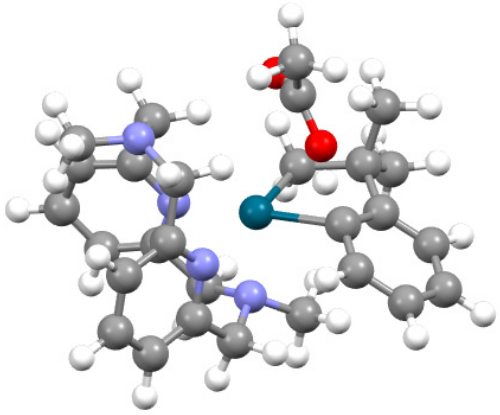

71

κ^3-MeN4Pd^{III}NeophylOAc-TS

Pd	10.121700	12.135300	3.649600
C	8.300700	11.110900	4.157600
C	8.297800	9.695200	4.249100
C	7.595900	9.042400	5.266300
C	6.898400	9.808800	6.220300
C	6.915600	11.212200	6.170400
C	7.619400	11.873000	5.153100
C	7.711400	13.382600	5.027200
C	9.130600	13.726400	4.526000
C	6.641500	13.854100	4.021400
C	7.473100	14.112400	6.360500
H	8.818300	9.117900	3.485800
H	7.578300	7.958100	5.318800
H	6.345600	9.307900	7.010300
H	6.388800	11.780000	6.933200
H	9.803100	14.004800	5.349800
H	9.135800	14.502700	3.746700
H	5.641200	13.548900	4.358000
H	6.827200	13.446100	3.021200
H	6.663600	14.950500	3.947700
H	8.147300	13.748800	7.147900
H	6.437300	13.986000	6.702700
H	7.650800	15.187300	6.225000
N	11.450600	10.565300	2.810000
N	11.914900	13.223900	3.332600
N	11.453500	12.522500	0.086300
N	11.282500	11.515800	5.511400

C	12.237400	9.988100	3.755600
C	13.363600	9.237900	3.409000
C	13.675100	9.075000	2.051800
C	12.866900	9.687000	1.087400
C	11.762700	10.453600	1.493900
C	10.916800	11.217200	0.493900
C	11.276200	13.676400	0.979600
C	12.265400	13.746000	2.127300
C	13.548300	14.283300	1.945000
C	14.478900	14.229700	2.988700
C	14.111600	13.636600	4.203100
C	12.813000	13.143400	4.349400
C	12.347400	12.556800	5.653100
C	11.810700	10.152700	5.187400
C	10.488200	11.444500	6.766300
C	12.701200	12.486700	-0.671800
H	13.974900	8.794000	4.187300
H	14.538300	8.489500	1.754200
H	13.079200	9.583000	0.028100
H	10.816200	10.604200	-0.411900
H	9.920000	11.363400	0.927200
H	10.244500	13.663400	1.358900
H	11.402700	14.583100	0.372600
H	13.801500	14.728300	0.988000
H	15.477500	14.631300	2.855500
H	14.810400	13.555400	5.028500
H	13.200300	12.140000	6.207300
H	11.928100	13.366600	6.263600
H	10.998400	9.442700	5.390900
H	12.642000	9.913800	5.865700
H	10.049300	12.421900	6.984500
H	11.142100	11.150800	7.601200
H	9.691400	10.703900	6.659200
H	12.621600	11.732400	-1.464500
H	12.869700	13.464400	-1.140200
H	13.595900	12.245800	-0.066900
O	8.098100	13.459300	1.028700
C	7.640400	12.305400	0.764600
O	7.639300	11.302200	1.613900
C	7.101200	11.987200	-0.613600
H	6.253200	11.299600	-0.552300
H	6.810200	12.902300	-1.135700
H	7.893400	11.493400	-1.192300
H	8.127400	11.427100	2.938200

IV

Energy (+ AcOH): -1584.174858 Hartrees

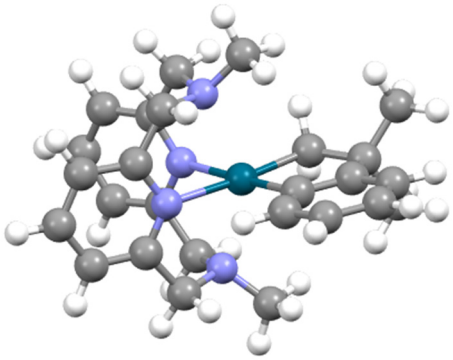

63

MeN4Pd^{III}Cycloneophyl

Pd	10.359900	11.731500	3.482400
N	11.994500	10.621500	2.579200
N	11.921000	13.216800	3.413100
N	10.321000	12.457700	1.185600
N	11.779500	11.153000	5.366500
C	12.959200	10.138900	3.396100
C	14.203600	9.756300	2.881900
H	14.967300	9.368700	3.547800
C	14.441100	9.907300	1.507800
H	15.400700	9.626100	1.087200
C	13.445600	10.455500	0.685700
H	13.614800	10.617300	-0.373600
C	12.220800	10.815300	1.259000
C	11.086100	11.406200	0.458000
H	11.466500	11.795800	-0.499400
H	10.376800	10.600000	0.227700
C	11.007500	13.779800	1.225000
H	10.251100	14.522700	1.509900
H	11.381400	14.054100	0.226100
C	12.130900	13.842400	2.229600
C	13.332500	14.513800	1.980600
H	13.487100	15.006300	1.026500
C	14.326400	14.510600	2.969900
H	15.271000	15.014600	2.794900
C	14.107500	13.821800	4.171800
H	14.871200	13.771200	4.940600
C	12.884500	13.169400	4.363200
C	12.559400	12.397800	5.617300
H	13.485500	12.172700	6.169500

H	11.939000	13.037400	6.259400
C	12.604800	10.021300	4.857500
H	12.007200	9.109100	4.990000
H	13.520600	9.908200	5.459000
C	8.959700	12.592100	0.620900
H	8.443700	11.628500	0.683200
H	8.992500	12.915200	-0.432200
H	8.395000	13.330600	1.199500
C	11.051100	10.745300	6.589000
H	10.415000	11.570200	6.924900
H	11.748000	10.480600	7.401400
H	10.419700	9.879100	6.366000
C	8.876800	10.362000	3.493800
C	9.022900	9.054200	2.987000
H	9.988600	8.715400	2.612200
C	7.927800	8.170900	2.955900
H	8.053300	7.164800	2.562300
C	6.674200	8.590600	3.432000
H	5.825800	7.911600	3.406500
C	6.522100	9.888600	3.946000
H	5.550700	10.208900	4.322800
C	7.613300	10.777300	3.981400
C	7.523200	12.172500	4.568500
C	8.849100	12.919000	4.251700
H	9.254000	13.430700	5.141200
H	8.703300	13.667900	3.454000
C	6.338000	12.960200	3.977600
H	5.376300	12.489400	4.223800
H	6.419100	13.025100	2.883200
H	6.326800	13.982200	4.382600
C	7.330000	12.064300	6.094400
H	8.163000	11.515500	6.555400
H	6.397900	11.535300	6.338000
H	7.282600	13.065700	6.545600

IX. References

1. Bottino, F.; Di Grazia, M.; Finocchiaro, P.; Fronczek, F. R.; Mamo, A.; Pappalardo, S., Reaction of Tosylamide Monosodium Salt with Bis(halomethyl) Compounds: an Easy Entry to Symmetrical N-tosylazamacrocycles. *Journal of Organic Chemistry* **1988,** *53* (15), 3521-9.
2. Smith T. W, J., .Sellas T. J. , Neophyl Chloride. *Org. Synth. Coll.* **1952,** *32*, 90.
3. Gutiérrez, E.; Nicasio, M. C.; Paneque, M.; Ruiz, C.; Salazar, V., Synthesis and reactivity of new palladium alkyl complexes containing PMe3 ligands: Insertion reactions and formation of bis(pyrazolyl)borate derivatives. *J. Organomet. Chem.* **1997,** *549* (1–2), 167-176.
4. Campora, J.; Lopez, J. A.; Palma, P.; del Rio, D.; Carmona, E.; Valerga, P.; Graiff, C.; Tiripicchio, A., Synthesis and Insertion Reactions of the Cyclometalated Palladiumâˆ'Alkyl Complexes Pd(CH2CMe2-o-C6H4)L2. Observation of a Pentacoordinated Intermediate in the Insertion of SO2. *Inorg. Chem.* **2001,** *40* (17), 4116-4126.
5. Endo, K.; Grubbs, R. H., Chelated Ruthenium Catalysts for Z-Selective Olefin Metathesis. *J. Am. Chem. Soc.* **2011,** *133* (22), 8525-8527.
6. Gottlieb, H. E.; Kotlyar, V.; Nudelman, A., NMR Chemical Shifts of Common Laboratory Solvents as Trace Impurities. *Journal of Organic Chemistry* **1997,** *62* (21), 7512-7515.
7. Tang, F.; Zhang, Y.; Rath, N. P.; Mirica, L. M., Detection of Pd(III) and Pd(IV) Intermediates during the Aerobic Oxidative C-C Bond Formation from a Pd(II) Dimethyl Complex. *Organometallics* **2012,** *31* (18), 6690-6696.
8. Gaussian 16, Revision C.01, Frisch, M. J.; Trucks, G. W.; Schlegel, H. B.; Scuseria, G. E.; Robb, M. A.; Cheeseman, J. R.; Scalmani, G.; Barone, V.; Petersson, G. A.; Nakatsuji, H.; Li, X.; Caricato, M.; Marenich, A. V.; Bloino, J.; Janesko, B. G.; Gomperts, R.; Mennucci, B.; Hratchian, H. P.; Ortiz, J. V.; Izmaylov, A. F.; Sonnenberg, J. L.; Williams-Young, D.; Ding, F.; Lipparini, F.; Egidi, F.; Goings, J.; Peng, B.; Petrone, A.; Henderson, T.; Ranasinghe, D.; Zakrzewski, V. G.; Gao, J.; Rega, N.; Zheng, G.; Liang, W.; Hada, M.; Ehara, M.; Toyota, K.; Fukuda, R.; Hasegawa, J.; Ishida, M.; Nakajima, T.; Honda, Y.; Kitao, O.; Nakai, H.; Vreven, T.; Throssell, K.; Montgomery, J. A., Jr.; Peralta, J. E.; Ogliaro, F.; Bearpark, M. J.; Heyd, J. J.; Brothers, E. N.; Kudin, K. N.; Staroverov, V. N.; Keith, T. A.; Kobayashi, R.; Normand, J.; Raghavachari, K.; Rendell, A. P.; Burant, J. C.; Iyengar, S. S.; Tomasi, J.; Cossi, M.; Millam, J. M.; Klene, M.; Adamo, C.; Cammi, R.; Ochterski, J. W.; Martin, R. L.; Morokuma, K.; Farkas, O.; Foresman, J. B.; Fox, D. J. Gaussian, Inc., Wallingford CT, 2016.
9. Zhao, Y.; Truhlar, D. G., The M06 suite of density functionals for main group thermochemistry, thermochemical kinetics, noncovalent interactions, excited states, and transition elements: two new functionals and systematic testing of four M06-class functionals and 12 other functionals. *Theor. Chem. Acc.* **2008,** *120* (1-3), 215-241.
10. Andrae, D.; Haussermann, U.; Dolg, M.; Stoll, H.; Preuss, H., Energy-Adjusted Abinitio Pseudopotentials for the 2nd and 3rd Row Transition-Elements. *Theor. Chim. Acta* **1990,** *77* (2), 123-141.
11. Marenich, A. V.; Cramer, C. J.; Truhlar, D. G., Universal Solvation Model Based on Solute Electron Density and on a Continuum Model of the Solvent Defined by the Bulk Dielectric Constant and Atomic Surface Tensions. *J. Phys. Chem. B* **2009,** *113* (18), 6378-6396.